Development 127, 4277-4291 (2000)
Printed in Great Britain © The Company of Biologists Limited 2000
DEV2585

Effect of single and compound knockouts of estrogen receptors α (ERα) and β (ERβ) on mouse reproductive phenotypes

Sonia Dupont*, Andrée Krust*, Anne Gansmuller, Andrée Dierich, Pierre Chambon‡ and Manuel Mark

Institut de Génétique et de Biologie Moléculaire et Cellulaire, CNRS/INSERM/ULP, Collège de France, BP 163, 67404 Illkirch-Cedex, France

*These authors contributed equally to this work

‡Author for correspondence (e-mail: chambon@igbmc.u-strasbg.fr)

Accepted 14 July; published on WWW 7 September 2000

SUMMARY

The functions of estrogen receptors (ERs) in mouse ovary and genital tracts were investigated by generating null mutants for ERα (ERαKO), ERβ (ERβKO) and both ERs (ERαβKO). All ERαKO females are sterile, whereas ERβKO females are either infertile or exhibit variable degrees of subfertility. Mast cells present in adult ERαKO and ERαβKO ovaries could participate in the generation of hemorrhagic cysts. Folliculogenesis proceeds normally up to the large antral stage in both ERαKO and ERβKO adults, whereas large antral follicles of ERα$^{+/-}$/ERβKO and ERαβKO adults are markedly deficient in granulosa cells. Similarly, prematurely developed follicles found in prepubertal ERαKO ovaries appear normal, but their ERαβKO counterparts display only few granulosa cell layers. Upon superovulation treatment, all prepubertal ERαKO females form numerous preovulatory follicles of which the vast majority do not ovulate. The same treatment fails to elicit the formation of preovulatory follicles in half of the ERβKO mice and in all ERα$^{+/-}$/ERβKO mice. These and other results reveal a functional redundancy between ERα and ERβ for ovarian folliculogenesis, and strongly suggest that (1) ERβ plays an important role in mediating the stimulatory effects of estrogens on granulosa cell proliferation, (2) ERα is not required for follicle growth under wild type conditions, while it is indispensable for ovulation, and (3) ERα is also necessary for interstitial glandular cell development. Our data also indicate that ERβ exerts some function in ERαKO uterus and vagina. ERαβKO granulosa cells localized within degenerating follicles transform into cells displaying junctions that are unique to testicular Sertoli cells. From the distribution pattern of anti-Müllerian hormone (AMH) in ERαβKO ovaries, it is unlikely that an elevated AMH level is the cause of Sertoli cell differentiation. Our results also show that cell proliferation in the prostate and urinary bladder of old ERβKO and ERαβKO males is apparently normal.

Key words: Knockout mice, Functional redundancy, Ovary, Uterus, Prostate, Anti-Müllerian hormone, Sertoli cells, Mast cells, Estrogen receptors

INTRODUCTION

Estrogens regulate a wide variety of physiological processes in classical targets as the reproductive tract and gonads, as well as in nonreproductive tissues such as the skeletal and cardiovascular systems (for review and references see Couse and Korach, 1999). Two estrogen receptors (ERs) are known to transduce estrogenic signals: ERα (Green et al, 1986) and ERβ (Kuiper et al., 1996; Mosselman et al., 1996; Tremblay et al., 1997). The domain organization of ERα (Krust et al., 1986; Gronemeyer and Laudet, 1995) is conserved in ERβ (Muramatsu and Inoue, 2000, and references therein). In both ERα and ERβ, the nonconserved N-terminal A/B domain harbors a ligand-independent transactivation function AF1, that can be activated through mitogen-activated protein kinase-mediated phosphorylation of serine residues (Kato et al., 1995; Tremblay et al., 1997). The highly conserved C domain (the DNA-binding domain, DBD) of ERα and ERβ is responsible for their specific binding to estrogen response elements of target genes. The less conserved E domain that contains the ligand-binding domain (LBD), also contributes to receptor dimerization and harbors the AF2 ligand-dependent transactivation function (for Refs see Couse and Korach, 1999).

ERα and ERβ exhibit both differential and overlapping tissue distribution, and test-tube studies, as well as in vitro studies with transfected cultured cells, have revealed overlap, but also significant differences in their ligand-binding and transcriptional properties (for references see Couse and Korach, 1999; Saville et al., 2000). For example, the cell type- and promoter-dependent agonistic activity of 4-hydroxytamoxifen appears to be unique to ERα (Berry et al., 1990; Tremblay et al., 1997), whereas anti-estrogens that block the stimulatory activity of ERα/AP1 complexes appear to be potent agonists when bound to ERβ/AP1 complexes (Paech et al., 1997). Similarly, transactivation by ERα/Sp1 and ERβ/Sp1 complexes through Sp1 promoter elements is cell type-, ligand- and promoter-dependent (Saville et al., 2000).

Both ERα (Lubahn et al., 1993) and ERβ (Krege et al., 1998)

genes have been previously disrupted by targeted mutagenesis (αERKO and βERKO mutant mice, see Couse and Korach, 1999). Both disruptions lead to pleiotropic effects, but the αERKO and βERKO phenotypes are mostly distinct. It is, however, unclear whether the mutation generated by disruption of the gene for ERα in αERKO mice actually represents a null mutation, as a transcriptionally active form of ERα truncated for the A/B domain is present in low amounts in these mice (Couse et al., 1995). Because we wish to characterize in vivo the individual role of the AF1 and AF2 activation functions of ERα and ERβ, with respect to their estrogen- and anti-estrogen dependence, their target genes, their phosphorylation and their function in the stimulatory activity of ER/AP1 and ER/Sp1 complexes (see above), we have decided to generate new ERα- and ERβ-null mutant mice, that would serve as references for future genetic dissection of ERα and ERβ functional domains. We report here the generation of mice that fully lack ERα (ERαKO mutants), ERβ (ERβKO mutants), or both ERα and ERβ (ERαβKO mutants), and the comparison of their reproductive tract and gonad phenotypes with those of the previous αERKO, βERKO and αβERKO (Couse et al., 1999b) mutants.

MATERIALS AND METHODS

Generation of ERα null mutant mice (ERαKO)

Mouse ERα (mERα) genomic clones were obtained by screening a 129/Sv embryonic stem (ES) cell DNA library, with a mERα cDNA probe (nucleotide 177 to 2007; White et al., 1987). A targeting vector was generated from a 9 kb *Bam*HI fragment containing exon 3 (nucleotide 655 to 845, amino acids 156-218; White et al., 1987) encoding the first zinc finger of the DBD (Fig. 1a). The TKneo cassette from pHR56 (Metzger et al., 1995) was cloned into the *Eco*47III site, and a loxP site followed by a *Bam*HI site were introduced at the *Nhe*I site by PCR-based site-directed mutagenesis (Fig. 1a). The 10 kb *Pml*I-*Hpa*I fragment of the targeting vector (Fig. 1a) was electroporated into 129/SvPas H1 ES cells (Dierich and Dollé, 1997) and G418 neomycin-resistant clones were expanded (Lufkin et al., 1991).

ES cells containing a targeted ERα^{L3} allele were identified by Southern blot analysis of *Bam*HI-digested ES cell genomic DNA, using 5′ (P5′) and 3′ (P3′) external probes and a 'neo' probe (Fig. 1a). Targeted ES cells were injected into C57BL/6 blastocysts and returned to a pseudopregnant host of the same strain. Chimeric males were obtained that transmitted the mutation through crosses with C57BL/6 females, yielding heterozygous ERα$^{L3/+}$ mice (mice with a L3 allele and a WT(+) allele). ERα$^{L3/+}$ mice were bred with homozygous CMV-Cre transgenic mice (Dupé et al., 1997) to generate ERα$^{L-/+}$ mice (mice bearing one allele in which exon 3 and the selectable marker were deleted), as well as ERα$^{L2/+}$ mice (mice bearing one floxed allele in which exon 3 is flanked by loxP sites) (see Fig. 1a). Inbreeding of ERα$^{L-/+}$ mice yielded ERα$^{L-/L-}$ (also designated as ERα$^{-/-}$ or ERαKO) mice homozygous for the deletion of ERα exon 3, whereas inbreeding of ERα$^{L2/+}$ mice yielded homozygous conditional 'floxed' ERα$^{L2/L2}$ mice.

Genotyping on tail-biopsy DNA was performed by PCR using primers P1 (5′-TTGCCCGATAACAATAACAT-3′), P2 (5′-ATTGTCTCTTTCTGACAC-3′) and P3 (5′-GGCATTACCACTTCTCCTGGGAGTCT-3′) (see Fig. 1a; targeted allele). The size of P1-P2 and P1-P3 fragments from WT is 364 and 889 bp, respectively, and that of the P1-P3 fragment from the ERα^{L-} allele is 359 bp.

Generation of ERβ null mutant mice (ERβKO)

A 15 kb genomic clone containing exons 2-4 of the gene for ERβ (Fig. 1d) was isolated from the above ES cell genomic DNA library using two 5′-radiolabeled oligonucleotides, 5′-ATGACATTCTACAGTCCTGCTGTGATG-3′ (nucleotides 424 to 450) and 5′-GAAGTGAGCATCCCTCTTTGCGTTTGG-3′ (nucleotides 732 to 706), corresponding to sequences of the rat ERβ A/B region (Kuiper et al., 1996). The 6.8 kb *Nhe*I-*Eco*RI fragment containing exon 3 (nucleotides 239 to 411; amino acids 77 to 134; Tremblay et al., 1997) encoding the first zinc finger of the DBD was used to generate a targeting vector. The NEO fragment, derived from pKJ-I (Adra et al., 1987) was introduced in the 5′ to 3′ orientation into exon 3 *Spe*I site. ES cell electroporation was performed as above. To identify ES cells containing a targeted allele, ES cell DNA was digested with *Xba*I and hybridized with 5′ and 3′ probes (P5′ and P3′), and a neo probe (Fig. 1d).

Inbreeding of heterozygotes, that were obtained as described above, yielded homozygotes for ERβ disruption within exon 3 (ERβ$^{-/-}$ or ERβKO mice). Tail DNA genotyping was accomplished by PCR using primers P1 (5′-TATCCCTAGCTCTGGAAGGC-3′), P2 (5′-ACATTTATATCAGATCATCTCTGC-3′) and P3 (5′-AAGCGCATGCTCCAGACTGC-3′) (Fig. 1d, targeted allele), that yield a 381 bp fragment for WT mice (P1 and P2 primers), a 237 bp fragment for homozygous mutants (primers P1 and P3), and both fragments for heterozygotes.

Analysis of ERα and ERβ transcripts

Total RNA was extracted from uterus (ERα) or ovaries (ERβ) as described (Auffray and Rougeon,1980). Reverse transcription was carried out on 1 μg of total RNA with M-MuLV reverse transcriptase (Biolabs). Subsequent nested PCR was performed to amplify full-length coding cDNAs of ERα (1.8 kb) and ERβ (1.65 kb). In the case of ERα, two sets of primers (coordinates as in White et al., 1987) were used: set 1 primers (30 cycles), A 5′-CGGCTGCCACTTACCATGACCA-3′ (nucleotides 176-194) and A′ 5′-GGGGAGCCTGGGAGCTCTCAGAT-3′ (nucleotides 1986-2007); set 2 primers (30 or 45 cycles), B 5′-ACCATGACCATGACCCTTCACA-3′ (nucleotides 188-209) and B′ 5′-CTCTCAGATCGTGTTGGGGAAG-3′ (nucleotides 1973-1994). In the case of ERβ: set 1 primers, A 5′-TCTCTGAGAGCATCATGTCC-3′ and A′ 5′-CAGCCTGGCCGTCACTGTGA-3′; set 2 primers, B 5′-TGCTCTAGACCACCATGTCCATCTGTGCCTCT-3′ and B′ 5′-CCGGAATTCTCACTGTGACTGGAGGTTCTG-3′ (Tremblay et al., 1997, GenBank AF067422 and S. D., unpublished data), were used. The ERβ amplified products were analyzed by Southern blotting with four 5′-radiolabeled oligonucleotides specific for ERβ exons 3, 4, 5 and 6, and by sequencing.

ERα western blotting

Protein extracts were prepared from WT and ERαKO uterus according to Rochette-Egly et al. (1994). 50 μg of protein were separated on 10% gel by SDS-PAGE and transferred onto nitrocellulose membrane. ERα was detected with a rabbit polyclonal antibody (MC20, Santa Cruz Biotechnology). The same blot was hybridized with an anti-actin antibody used as internal control.

Immunohistochemistry

Immunoperoxidase labeling for detection of ERβ was performed on frozen sections of ovaries, postfixed in Zamboni's fluid, using a polyclonal antibody raised against a peptide corresponding to residues 467-485 (Tremblay et al., 1997) of the ERβ region F. Immunoperoxidase labeling for detection of AMH was carried out on histological sections from ovaries fixed in Bouin's fluid and embedded in paraffin (Al-Attar et al., 1997). The sections were counterstained with Harris' Haematoxylin. Cell proliferation was assessed by immunoperoxidase labeling on histological sections from paraformaldehyde-fixed, paraffin-embedded prostates using the antibody NCL-Ki67p (Novocastra Laboratories). Peroxydase activity was revealed using 4-chloro-1-naphthol (Merck) as a substrate (nuclei counterstained with DAPI).

Bromodeoxyuridine (BrdU) incorporation into DNA

12- and 20-month-old ERβKO and control males (WT and ERβ$^{+/-}$) as well as 8-month-old ERαβKO and control males (ERβ$^{+/-}$ and ERα$^{+/-}$) were injected intra-peritoneally (IP) four times every 2 hours with 10 mg BrdU/kg of body weight and sacrificed 2 hours after the last injection. Prostates were fixed in Bouin's fluid for 16 hours at 4°C, embedded in paraffin and BrdU incorporation revealed using a anti-BrdU mouse monoclonal antibody (Boehringer Mannheim) and immunoperoxidase labeling (nuclei counterstained with Haematoxylin). BrdU-labeled nuclei were quantitated by counting at least 2000 nuclei.

Fertility of ER mutant mice

Young females (7-15 weeks old) and fertile males were bred during 15 weeks. The presence of seminal plugs, the number of pups per litter and the number of litters per female were scored. Male fertility was similarly tested by breeding young males and fertile females.

Superovulation and oocyte quantification

21- to 25-day-old wild-type and ER mutant females were injected IP with 10 units of PMSG (Folligon®-Intervet) followed by 5 units of human chorionic gonadotropin (hCG; Chorulon®-Intervet) 48 hours later, and sacrified 19-22 hours after the hCG injection. Oocyte/cumulus masses were extracted from oviducts, and oocytes were counted after enzymatic dissociation from the surrounding cumulus with hyaluronidase (37°C, 1 hour; Hogan et al., 1994). Ovaries were fixed in Bouin's fluid for histology.

RESULTS

Generation of ERα and ERβ single and double null mutant mice (ERαKO, ERβKO and ERαβKO)

We targeted exon 3 that encodes the first zinc finger of the DBD to generate a fully disrupted ERα mutant. The homologous recombination targeting vector (Fig. 1a) was designed with three loxP sites flanking exon 3 and the TKneo cassette (see Fig. 1a, and Materials and Methods). Complete Cre recombinase-mediated excision of exon 3 and 'floxed' cassette in the L3 allele (Fig. 1a) should result in the creation of a stop codon at the new amino acid position 158 generated by splicing exon 2 and 4 transcripts (White et al., 1987; Couse et al., 1995; A. K., unpublished). Thus, the putative truncated protein produced from the deleted allele (L-) would be 157 amino acids long, lacking the C to F regions of ERα. However, partial Cre-mediated excision of the 'floxed' selection cassette should yield the conditional 'floxed' allele L2 (Fig. 1a).

Chimeric males derived from targeted L3 ES clones transmitted the mutation through their germline. Inbreeding of heterozygous ERα$^{L-/+}$ (see Materials and Methods) yielded ERα$^{L-/L-}$ mice in accordance with Mendelian expectation. The full disruption of the gene for ERα was confirmed by the absence in ERαKO uterus of any ERα polypeptide immunoreacting with an antibody directed against the F region of ERα (Fig. 1b). Moreover, no ERαRNA containing transcripts of any of the exons located downstream of exon 2 could be detected by RT-PCR (Fig. 1c, and data not shown). Collectively, these results demonstrate that the ERα$^{L-/L-}$ mice are indeed ERα null mutants that we also designated as ERα$^{-/-}$ or ERαKO mutants. Note that in the previously generated mouse αERKO mutant, ERα was disrupted by inserting a *neo* gene into exon 2 (Lubahn et al., 1993). No full-length ER mRNA could be detected, but one smaller transcript variant encoded a truncated ERα protein still possessing the DBD and the LBD of wild-type (WT) ERα, as well as significant estrogen-dependent transcriptional capacity (see Couse et al., 1995).

The mouse gene for ERβ was disrupted through homologous recombination by inserting the *neo* gene into the *Spe*I site of exon 3, which encodes the first zinc finger of the DBD (Fig. 1d, and Materials and Methods). Chimeric males derived from targeted ES cell clones transmitted the mutation through crosses with C57BL/6 females. Inbreeding of heterozygote mice yielded a Mendelian distribution of all expected genotypes. To establish that ERβ was actually lacking in these mutants, we first examined ERβ transcripts using RT-PCR performed on total RNAs extracted from ERβ$^{+/+}$ and ERβ$^{-/-}$ adult mouse ovaries (Fig. 1e; see Materials and Methods). The expected 1.6 kb cDNA species was obtained with WT RNAs, but not with ERβ$^{-/-}$ RNAs, which yielded three fainter cDNA species (ERβ$^{-/-}$ 1 to 3, Fig. 1e). Their analysis showed that they represent different alternative splicings of ERβ transcripts (Fig. 1e). All three lacked exon 3, thus leading through splicing of exon 2 and 4 transcripts to a frameshift with the creation of two stop codons at the beginning of exon 4 (nucleotide position 416 to 421 in Tremblay et al., 1997) and resulting in a putative 77 amino acid long peptide. Only the targeted exon 3 transcript was spliced out in ERβ$^{-/-}$1, whereas the transcript of two additional exons (6 and 7) were spliced out in ERβ$^{-/-}$3. This alternative splicing of both (exons 6 and 7) transcripts has been described in normal mouse tissues (Lu et al., 1998). ERβ$^{-/-}$2 was not fully characterized, but must correspond to an additional splicing occurring downstream of exon 6. Note that in the previously reported similar, but not identical, disruption of the gene for mouse ERβ (βERKO; Krege et al., 1998), a PGK *neo* gene was inserted in the reverse orientation into exon 3 *Pst*I site (nucleotides 329-334, Tremblay et al., 1997), i.e., downstream of our insertion site, into the sequence encoding the first zinc finger of the DBD. Several similar, but not identical splicing variants were also found in this βERKO mutant, in which the exon 3 transcript was consistently spliced out. In two described transcripts, this splicing out generated the same frameshift and stop codons as in our ERβKO mutant, and resulted in the same putative truncated peptide that lacks both DBD and LBD. However, in the third described transcript, exon 3 and exon 4 splicing out resulted in an open reading frame yielding a putative polypeptide lacking the DBD.

Our disruption of the gene for mouse ERβ was also controlled by immunohistochemistry (Fig. 1f). No immunostaining could be detected on ERβ$^{-/-}$ ovary sections, while a clear signal was observed in WT granulosa cell nuclei. Thus, the above data indicate that our present ERβ disruption results in a null mutant (ERβ$^{-/-}$ or ERβKO) that is most probably functionally identical to the previous βERKO mutant (Krege et al., 1998).

ER double heterozygous mice (ERα$^{+/-}$/ERβ$^{+/-}$), obtained from breeding ERα$^{+/-}$ females with ERβ$^{-/-}$ males, were inbred to generate mutant mice homozygous for ERα and ERβ disruption, designated as ERαβKO. All genotypes were obtained in agreement to Mendelian expectation and with a normal sex ratio (data not shown).

Fertility of ERα and ERβ single and compound mutants

In continuous mating studies, our ERαKO and ERαβKO males

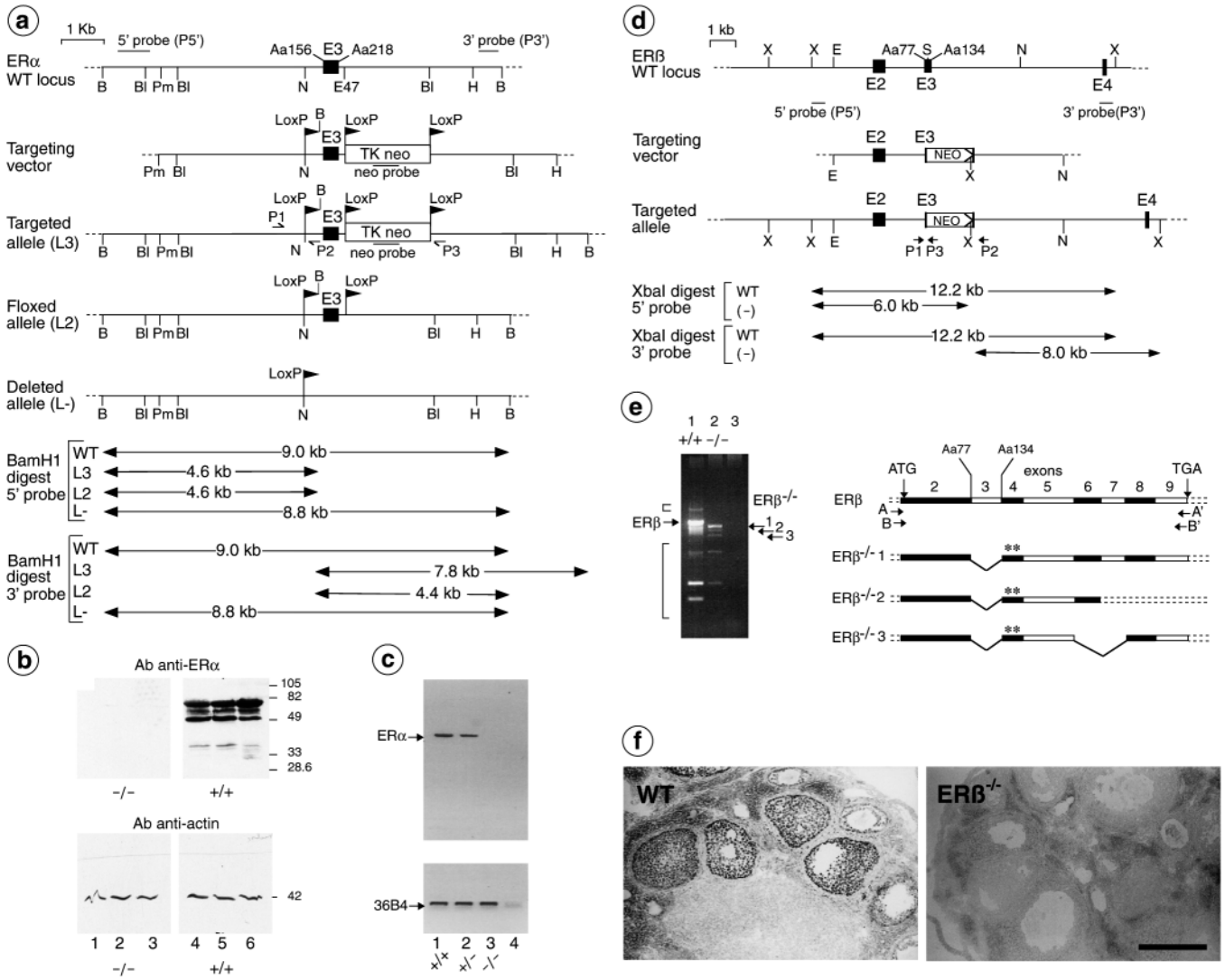

Fig. 1. Targeted disruption of mouse ER genes. (a) Schematic strategy to generate ERαKO mice: diagrams showing the wild-type (WT) ERα locus, the targeting vector, the targeted allele, the floxed allele and the deleted allele after Cre-mediated recombination. Exon 3 (E3) is shown as a black box. The location of P5′ and P3′ probes is indicated. B (*Bam*HI), Pm (*Pml*I), Bl (*Bgl*II), N (*Nhe*I), E47 (*Eco*47III), H (*Hpa*I). The TKneo cassette is shown and loxP sites indicated with black arrowheads. Arrows indicate the positions of PCR primers (P1, P2, P3) used for DNA genotyping. The size of restriction fragments obtained by Southern blot analysis is given in kilobases (kb). (b) Western blot analysis of ERα protein in WT and ERαKO uterus (see Materials and Methods). Note the lack of ERα immunoreactivity in ERαKO uterus (left of the top panel). The lower species on the right of the top panel correspond to degradation products of ERα. (Bottom panel) Actin immunoblotting used as internal control. Molecular weights are indicated. (c) Detection of mERα transcripts by RT-PCR (30 cycles) of WT, ERα$^{+/-}$ and ERα$^{-/-}$ uterus total RNAs. RT-PCR products were separated on agarose gel. Top: lanes 1, 2 and 3: WT, ERα$^{+/-}$ and ERα$^{-/-}$ RNAs, respectively; lane 4, no RNAs. No RT-PCR products could be detected in ERα$^{-/-}$ samples, by ethidium bromide staining or Southern blotting, irrespective of the number of PCR cycles (30 or 45, see Materials and Methods). Bottom: RT-PCR of 36B4 RNA used as an expression control. (d) Schematic strategy to generate ERβKO mice: diagrams showing the wild-type (WT) ERβ locus, the targeting vector and the targeted allele. Exons 2, 3 and 4 (E2, E3 and E4) are shown as black boxes. The location of P5′ and P3′ probes is indicated. X (*Xba*I), E (*Eco*RI), S (*Spe*I), N (*Nhe*I). The neomycin sequence is depicted as an open box (NEO). Mouse genotyping was carried out by PCR using primers (P1 to P3) shown by arrows. Southern blot analysis of *Xba*I-digested DNAs allows to distinguish WT and targeted alleles as indicated. (e) Detection of mouse ERβ transcripts by RT-PCR using total RNA from WT and ERβ$^{-/-}$ ovary. RT-PCR products separated on agarose gel (lane 1, WT RNAs; lane 2, ERβ$^{-/-}$ RNAs; lane 3, no reverse transcriptase) were obtained by using primers A, A′ and B, B′ indicated as arrows. The three distinct transcripts obtained with ERβ$^{-/-}$ RNA are indicated as ERβ$^{-/-}$1 to 3. The diagram shows that they correspond to alternative splicings of mERβ$^{-/-}$. Double asterisks indicate the presence of stop codons. Broken lines indicate that the sequence is unknown. Bracketed RT-PCR products are unspecific. (f) Immunohistochemical staining of ERβ in WT and ERβ$^{-/-}$ ovaries. Scale bar: 400 μm in F.

were infertile (data not shown) in accordance with previous αERKO (Eddy et al., 1996) and αβERKO (Couse et al., 1999b) data. However, as reported for βERKO males (Krege et al., 1998), our ERβKO, as well as ERα$^{+/-}$/ERβKO males, exhibited normal fertility (data not shown).

Continuous mating studies were also carried out in females

to investigate the reproductive consequences of ERα and ERβ mutations. In accordance with previous αERKO data (Lubahn et al., 1993), our ERαKO females were infertile as shown by the total absence of copulatory plugs and pregnancy (Table 1). In contrast, ERβKO females were either infertile or exhibited a reduced fertility, even though they presented vaginal plugs, indicating a normal sexual behaviour (data not shown). An analysis of 12 ERβKO females showed that three groups could be distinguished. Six females (A) were subfertile with a normal number of litters (3.17±0.17) and a reduced number of pups per litter (3.95±0.34), while three others (B) had a much more reduced fertility (one litter and 2.00±0.58 pups per litter) and the remaining three (C) were apparently infertile. Interestingly, disruption of one ERα allele in the ERβKO null background ($ERα^{+/-}$/ERβKO mutants) resulted in complete female infertility.

Table 1. ER mutant female fertility in continuous matings

Genotype	*n*	Litters	Pups	Pups per litter	Litters per female
WT,$ERβ^{+/-}$	22	68	462	6.79±0.31	3.09±0.15
ERαKO	6	0	0	–	0
ERβKO (A)	6	19	75	3.95±0.34*	3.17±0.17
ERβKO (B)	3	3	6	2.00±0.58‡	1.00±0.00§
ERβKO (C)	3	0	0	–	0
$ERα^{+/-}$/ERβKO	7	0	0	–	0

Control (WT, $ERβ^{+/-}$) and mutant females (7-15-week-old) were bred with fertile males for 15 weeks. The number of pups per litter and the number of litters per female were scored. ERβKO females responding differently are separated in three groups (A), (B) and (C). Results are presented as mean±s.e.m.

*Statistically different from control females, P=0.0001 (unpaired t-test).

‡,§Statistically different from ERβKO (A) females.

‡P=0.041 (unpaired t-test).

§P=0.0001 (unpaired t-test).

Genital tract phenotype of adult ERαβKO females

For each mutant genotype (ERαKO, ERβKO and ERαβKO), as well as for wild type (WT) age-matched 'controls', ovaries and genital tracts from at least three mice were analysed. The genital tracts of sexually mature ERβKO and $ERα^{+/-}$/ERβKO mice were similar to those of WT females. In contrast, ERαKO uterus and vagina were hypoplastic and did not display cyclic changes (Fig. 2a-c,e,g, and data not shown). In ERαβKO females, the lengths of the oviducts, uterine horns and vagina were normal, indicating that signaling through ERs is not required for the growth of the genital tract along the antero-posterior body axis (Fig. 2a,b). However, the diameter and wall thickness of the ERαβKO uterus and vagina were, on average, reduced twofold when compared with their ERαKO counterparts (Fig. 2a-h). The increased uterine and vaginal hypoplasia generated upon inactivation of the gene for ERβ in the ERαKO genetic background was equally distributed between epithelium, lamina propria and smooth muscles, and reflected decreases in both cell number and size (compare E, LP and M in Fig. 2e-h).

Structural analysis of adult ovaries of ERα and ERβ single and compound mutants

Ovaries of WT adult mice (OV, Fig. 2b) consist of a follicular and an interstitial compartments. The follicular compartment comprises primordial (PR, Fig. 3a), growing (e.g. A, Fig. 3a and c) and atretic follicles (not shown), as well as corpora lutea (CL, Fig. 3a). The interstitial

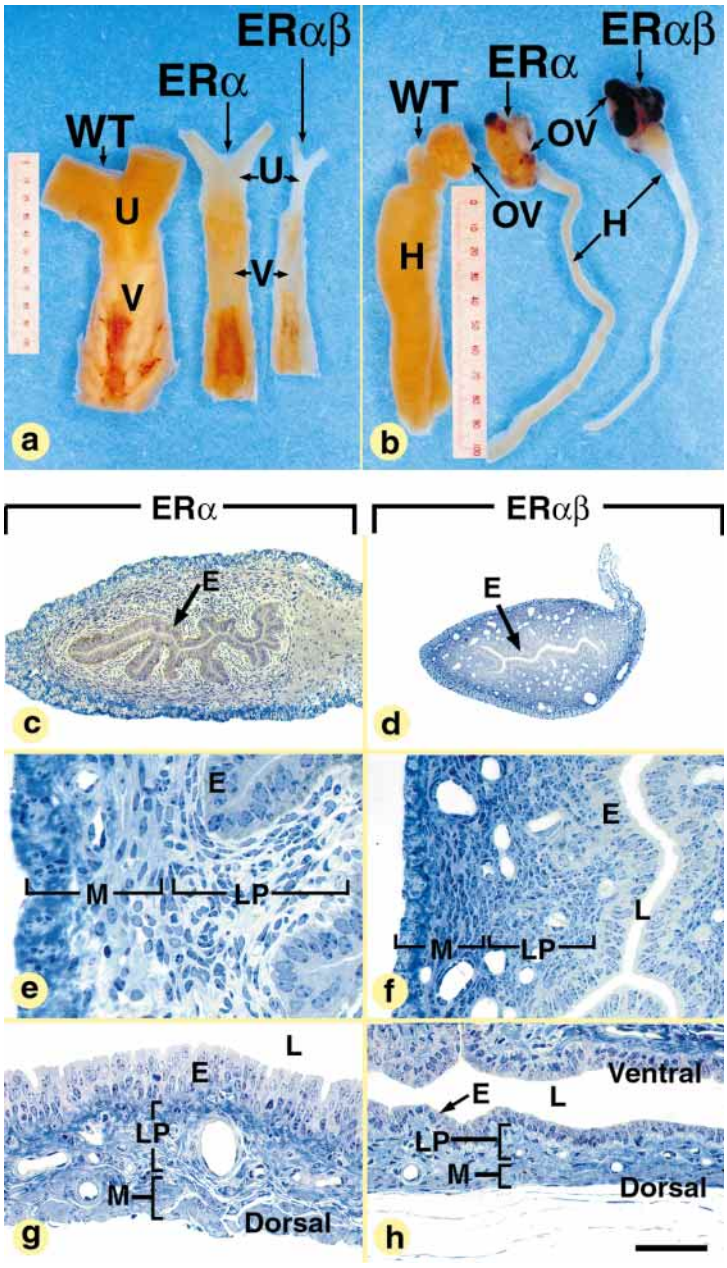

Fig. 2. Ovaries and genital tracts of 14-week-old WT, ERαKO (ERα) and ERαβKO (ERαβ) females. (a) Ventral views of the body of the uterus (U) and vagina (V); note that the vestibular (caudal) portion of the vagina was removed during dissection. (b) Ovaries (OV) and uterine horns (H). (c-h) Transverse semi-thin sections stained with toluidine blue at similar levels of uterine horns (c-f) and dorsal wall of the vagina (g and h). Note that ERαβKO vaginal epithelium is composed of two cell layers instead of four in its ERαKO counterpart and that there is conspicuous decrease in size of ERαβKO uterine and vaginal smooth muscle cells, which contain less myofibrils than their ERαKO counterparts. E, epithelium; L, lumen of the organ; LP, lamina propria; M, smooth muscles. Scale bars: 1 cm in a,b; 150 μm in c,d; 30 μm in e,f; 40 μm in g,h.

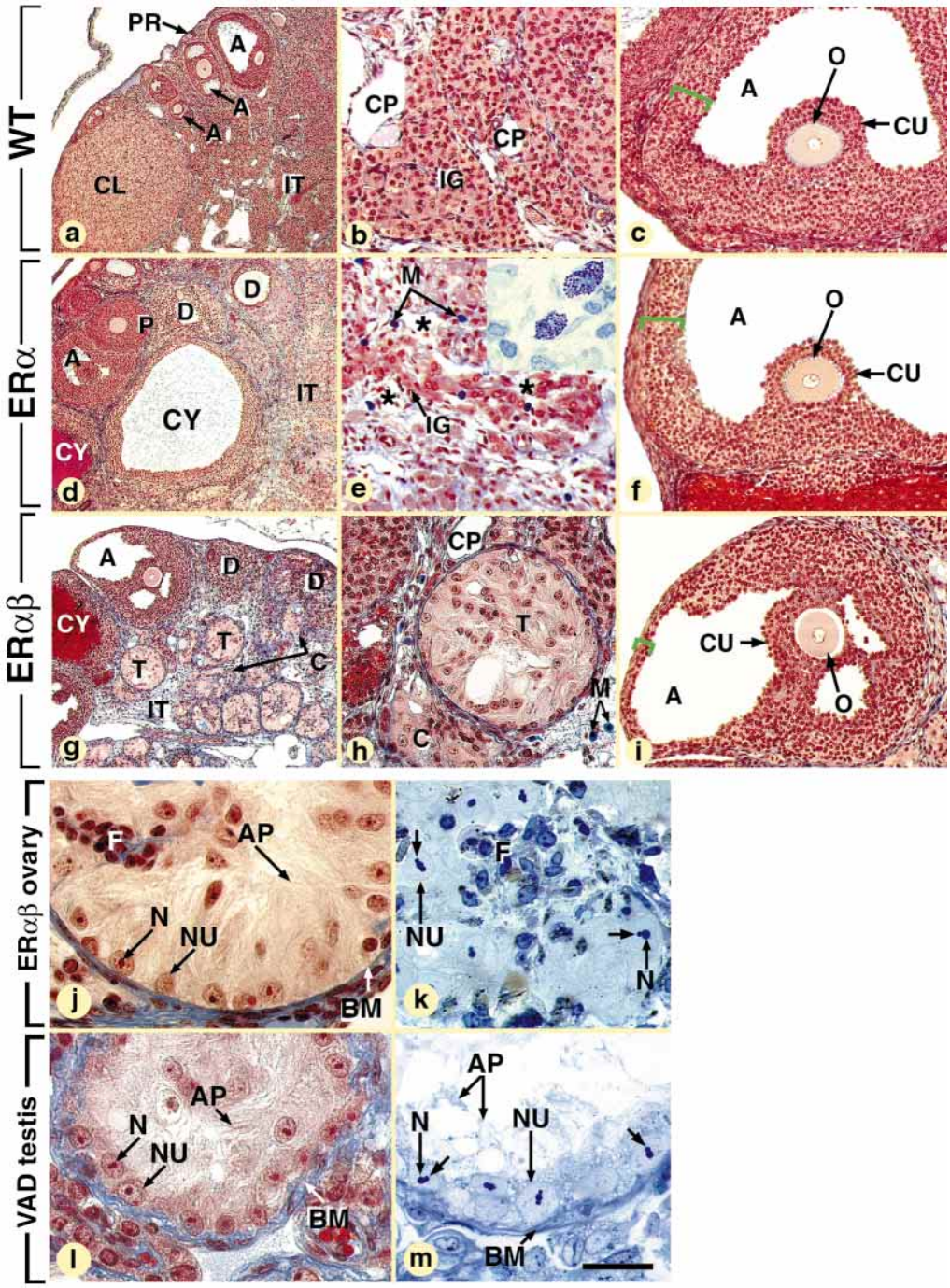

Fig. 3. Comparison of ovaries of 14-week-old WT, ERαKO (ERα) and ERαβKO (ERαβ) mice (a-i), and comparison of Sertoli cells in intra-ovarian tubules (j) or clusters (k) from adult ERαβKO (ERαβ) females and in testis seminiferous tubules from wild-type vitamin A-deficient (VAD) adult males (l,m). (a,d,g) Overview of the ovarian cortex and medulla. (b,e,h) High-power magnification of the medulla; the inset in (e) shows two mast cells metachromatically stained with toluidine blue. (c,f,i) Representative sections of large antral follicles. Note that (a-j,l) are histological sections from paraffin-embedded organs, while (k,m) are semi-thin sections. The asterisks in (e) indicate fluid-filled extracellular spaces between interstitial cells. The green brackets in (c,f,i) encompass the granulosa cell layers forming the wall of the ovarian follicle. The small arrows in panels (k) and (m) point to nucleolar satellites. Tetrachrome stain (a-j,l) and toluidine blue (k,m and inset in e). A, antrum; AP, apical Sertoli cell processes; BM, basement membrane; C, Sertoli cell clusters; CL, corpus luteum; CP, capillaries; CU, cumulus oophorus; CY, ovarian cysts; D, atretic (degenerating) follicles; F, fibroblastic cells; IG, interstitial glandular cells; IT, interstitial compartment; M, mast cells; NU and N, Sertoli cell nuclei and nucleoli, respectively; O, oocyte; P, primary follicle; PR, primordial follicles; T, Sertoli cell tubules. Scale bar: 255 μm in a,d,g; 65 μm in b,e,h; 100 μm in c,f,i; 30 μm in j,l; 25 μm in k,m.

compartment (IT, Fig. 3a) is most prominent in the ovarian medulla and consists of compact clusters of large glandular cells (IG, Fig. 3b), numerous fibroblasts, capillaries (CP, Fig. 3b) and rare mast cells (not shown). Adult ERβKO ovaries were macroscopically normal and showed normal antral follicles, but in most of them corpora lutea were scarce or absent (not shown). In contrast to Krege et al. (1998), we did not detect any increase in the number of atretic follicles in our ERβKO ovaries.

Ovaries from adult ERαKO mice (14-week- or 6-month-old) displayed (1) large, frequently hemorrhagic, cysts (Fig. 2b) originating from antral follicles (CY, Fig. 3d); (2) normal primordial, primary and antral follicles (e.g. P and A, Fig. 3d and f); (3) a large excess of follicles at advanced stages of atresia (D, Fig. 3d); (4) an absence of typical mature corpora lutea (Fig. 3d, and data not shown); and (5) a marked reduction in the number of glandular interstitial cells that appeared loosely arranged as a consequence of edema of the interstitial tissue (IG and asterisks in Fig. 3e). Moreover, numerous deep-blue-stained cells were scattered in the interstitial compartment of ERαKO ovaries (M, Fig. 3e), which contained dozens of granules staining metachromatically with toluidine blue (Fig. 3e, inset). These features are characteristic of mast cells (Fawcett, 1986).

A polycystic ovarian phenotype similar to that of ERαKO mice was observed in adult (14-week- and 6-month-old) ERαβKO mice (OV, Fig. 2b; CY, Fig. 3g, and data not shown). Components of the follicular compartment (including primordial, primary, small antral, degenerating and hemorrhagic cysts (CY and D, Fig. 3g, and data not shown)) and cellular composition of the interstitial compartment (e.g. M, Fig. 3h, and data not shown) were similar in ERαβKO and ERαKO ovaries. However, the largest antral follicles of ERαβKO ovaries were abnormal in that (1) their walls were locally very thin, owing to a lack of granulosa cells (A, Fig. 3g,i, and compare the green brackets in Fig. 3c,f,i); and (2) they never reached the size of their counterparts in WT and ERαKO ovaries (Fig. 3c,f,i).

Interestingly, disruption of only one allele of ERα from the ERβ null genetic background ($ERα^{+/-}$/ERβKO) resulted in ovaries that consistently lacked corpora lutea and displayed numerous abnormal antral follicles with similar characteristics to those of ERαβKO ovaries. However, $ERα^{+/-}$/ERβKO ovaries displayed no hemorrhagic cysts and showed a normal organization of interstitial glandular cells with rare mast cells (data not shown).

Strikingly, all ERαβKO ovaries, but none of the ERαKO and ERβKO single mutant ovaries, contained unusually large cells that exhibited an abundant cytoplasm, a pale 'dusty' chromatin and a prominent nucleolus and were organized into either irregular clusters (C, Fig. 3g,h; Fig. 3k) or short tubules (T, Fig. 3g,h; Fig. 3j). These cells, which were essentially observed in the ovarian medulla (although few of them were also detected in the ovarian cortex in association with follicles at advanced stages of atresia (D, Fig. 3g)), have no counterparts in normal mammalian ovaries (Harrison and Weir, 1977; Mossman and Duke, 1973). Based on morphological criteria described below, they were identified as fully differentiated Sertoli cells.

Presence of Sertoli cells in adult ERαβKO ovaries

Sertoli cells, which, under normal conditions, are found exclusively in testis seminiferous tubules (Figs 3l,m and 4b,e,h,i), are columnar cells attached to a basement membrane (BM, Fig. 3l,m) whose apexes possess numerous veil-like processes (AP, Fig. 3l,m) and whose nuclei are ovoid and located near the basement membrane (NU, Fig. 3l,m). These histological features are particularly conspicuous in seminiferous tubules depleted from their germ cells, such as those from vitamin A-deficient (VAD) mice (Ghyselinck et al., 1999; Fig. 3l,m).

When examined by high-resolution light microscopy and electron microscopy, Sertoli cells display characteristic nuclear profiles: the nuclear envelope exhibits deep and narrow indentations (not shown); and the prominent reticular nucleolus (N, Figs 3l,m and 4b) is characteristically fused to two large clumps of heterochromatin (or nucleolar satellites, small arrows in Figs 3m and 4b; Kuhn and Therman, 1988). Plasma membrane-cytoskeleton-endoplasmic reticulum complexes, known as ectoplasmic specializations, are unique to pubertal and postpubertal Sertoli cells. These are formed by regularly spaced belts of circumferential actin filaments (A, Fig. 4e,h,i) that are bordered on the cytoplasmic side by cisternae of endoplasmic reticulum (ER, Fig. 4e,h,i) and are surrounding a series of occluding junctions (J, Fig. 4e,h) connecting adjacent Sertoli cells (S1 and S2, Fig. 4h) (Pelletier and Byers, 1992; Weber et al., 1988; Byers et al., 1993). It is noteworthy that in both WT and ERαβKO ovaries, granulosa cells (G, Fig. 4d) are connected via gap junctions (GAP) and desmosomes (D), but not by occluding junctions, although they represent the female homologs of Sertoli cells, with respect to their embryological origin from the genital ridges (Swain and Lovell-Badge, 1999), their function of nurse cell for the germ-cell lineage and their gene expression pattern (see for example Couse et al., 1999b and references therein).

The abnormal cells found in the ovary of adult ERαβKO mutants were unambiguously identified as Sertoli cells based on the following criteria: (1) they were connected by typical ectoplasmic specializations indistinguishable from those observed in 2-week-old normal prepubertal testes (compare ER, A and J in Fig. 4c,f,g with 4e,h,i); (2) they displayed satellites flanking a large reticular nucleolus (N and small arrows in Figs 3j,k and 4a), as well as elongated and indented nuclear profiles (arrowhead in Fig. 4a); and (3) their spatial organization within ovarian tubules faithfully mimicked that of authentic Sertoli cells within germ-cell-free seminiferous tubules (compare Fig. 3j with 3l).

Structural analysis of ovaries from prepubertal and young pubertal mice

The follicular compartment of prepubertal, 23-day-old WT, ERβKO and $ERα^{+/-}$/ERβKO females contained only rare small antral follicles (A, Fig. 5a,c; SA, Fig. 6a; and data not shown). In contrast, some large antral follicles of normal structure were seen in prepubertal ERαKO ovaries (LA in Fig. 6b) and the vast majority of the growing follicles in prepubertal ERαβKO ovaries possessed a well-defined antrum (A compare Fig. 5a with 5b; SA, compare Fig. 6a with 6c). The structure of the ERαβKO antral follicles was abnormal as: (1) the granulosa cells either formed a single layer (black arrowheads in Fig. 5b,d) or appeared loosely organized owing to the presence of multiple small cavities filled with follicular fluid (Fig. 5b,d); (2) the theca cells always formed a single layer (versus 2 to 4 layers in WT, ERαKO and ERβKO follicles; compare green brackets in Fig. 5c,d and data not shown); and (3) in a majority of the follicles, the oocyte was completely separated from the follicular wall and floated in the follicular fluid (O, Fig. 5b,d).

Altogether, these results strongly suggest that the secretory activity of the follicles increases prior to the normal onset of puberty in both ERαKO and ERαβKO mice. Additionally, in ERαβKO ovaries the proliferation rate of theca cells was apparently diminished.

Sertoli-like cells were not detected in prepubertal (i.e., 23-day-old) ERαβKO ovaries. However, all ERαβKO ovaries at the onset of puberty (i.e., 30 days) displayed, essentially between the follicles, but also within some atretic follicles, clusters of densely packed cells with abundant cytoplasm, pale elongated nuclei and large reticular nucleoli (S, Fig. 5f,h,i,j), that had no counterparts in age-matched WT, ERαKO and ERβKO ovaries (e.g., Fig. 5e,g). These cells lacked indentations of the nuclear envelope and nucleolar satellites (Fig. 5j), but were connected by ectoplasmic specializations (Ac, ER and J, Fig. 5k) and thus resembled normal immature Sertoli cells (Byers et al., 1993). With few exceptions (e.g. Fig. 5f,h), the clusters of Sertoli cells located within the atretic

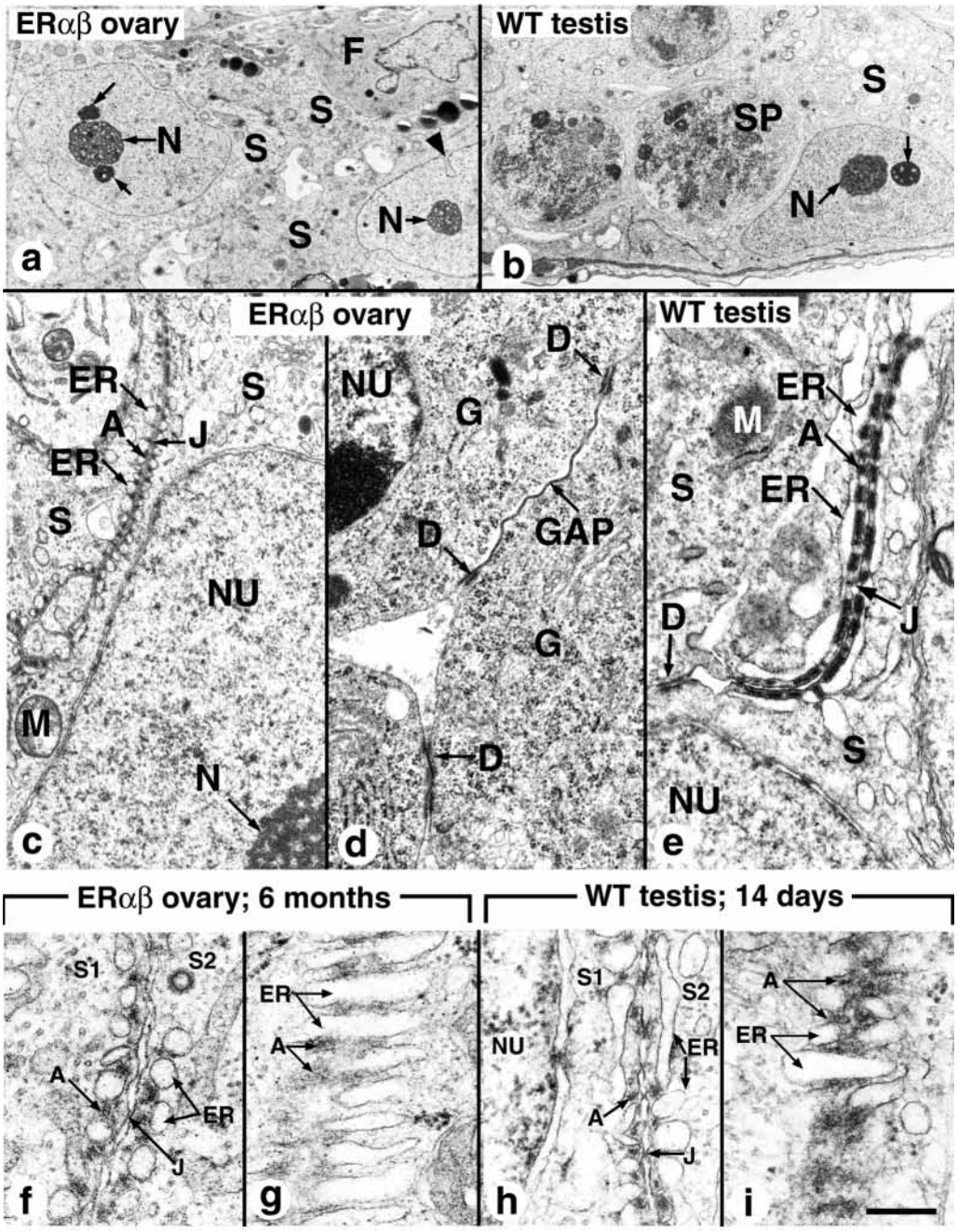

Fig. 4. Electron microscopic comparison of Sertoli-like cells in ERαβKO (ERαβ) ovaries, Sertoli cells in WT testes, and granulosa cells in ERαβKO ovaries, as indicated. (a-g) are from 6-month-old mice and (h,i) from a prepubertal male. Note that (f,h) are sections through adjacent Sertoli cells (S1 and S2), while (g) and (i) are sections through the cytoplasmic side of ectoplasmic specializations. Small arrows in panels (a) and (b) point to nucleolar satellites and the arrowhead to an indentation of nuclear envelope. A, bundles of actin microfilaments; D, desmosomes; ER, cisternae of endoplasmic reticulum at sites of ectoplasmic specializations; F, fibroblastic cell; G, granulosa cell; GAP, gap junction; J, occluding junctions; M, mitochondria; N, nucleoli; NU, nuclei; S, Sertoli cell; SP, spermatocytes. Scale bar: 4 μm in a,b; 0.5 μm in c-e; 0.25 μm in f-i.

ovarian follicles of peripubertal ERαβKO mice were small (two to five cells on average; Fig. 5i,j). The ectoplasmic specializations between extrafollicular Sertoli cells were identical to those observed in adult ovaries (see above), whereas those of intrafollicular Sertoli cells were less mature (Ac, ER and J in Fig. 5k). Therefore, although the vast majority of the Sertoli cells present in the ovaries of early post-pubertal and adult of ERαβKO mice are extrafollicular, they appear to arise, at least in part, within the epithelium of atretic follicles.

Expression of anti-Müllerian hormone (AMH) in ERαβKO ovaries

AMH expression is specific to Sertoli cells of the immature testis and granulosa cells of the adult ovary (Hirobe et al., 1992; Münsterberg and Lovell-Badge, 1991; and references therein), but its ectopic expression can induce the formation of seminiferous tubules in fetal ovaries (Vigier et al., 1987; Behringer et al., 1990). We used immunohistochemistry to investigate the possibility that overexpression of AMH in ERαβKO ovaries might promote the differentiation of Sertoli cells. In adult (i.e., 14-week-old) and early post-pubertal (i.e., 30-day-old) ERαβKO ovaries, AMH was detected in primary and in small antral follicles (P and SA, Fig. 7b-d) and was absent from granulosa cells of large antral and atretic follicles (LA and D, Fig. 7b,d,e). This distribution pattern of AMH was indistinguishable from that observed in age-matched WT ovaries (Ueno et al., 1989; Baarends et al., 1995; Fig. 7a, and data not shown). Moreover, follicles showing synthesis of

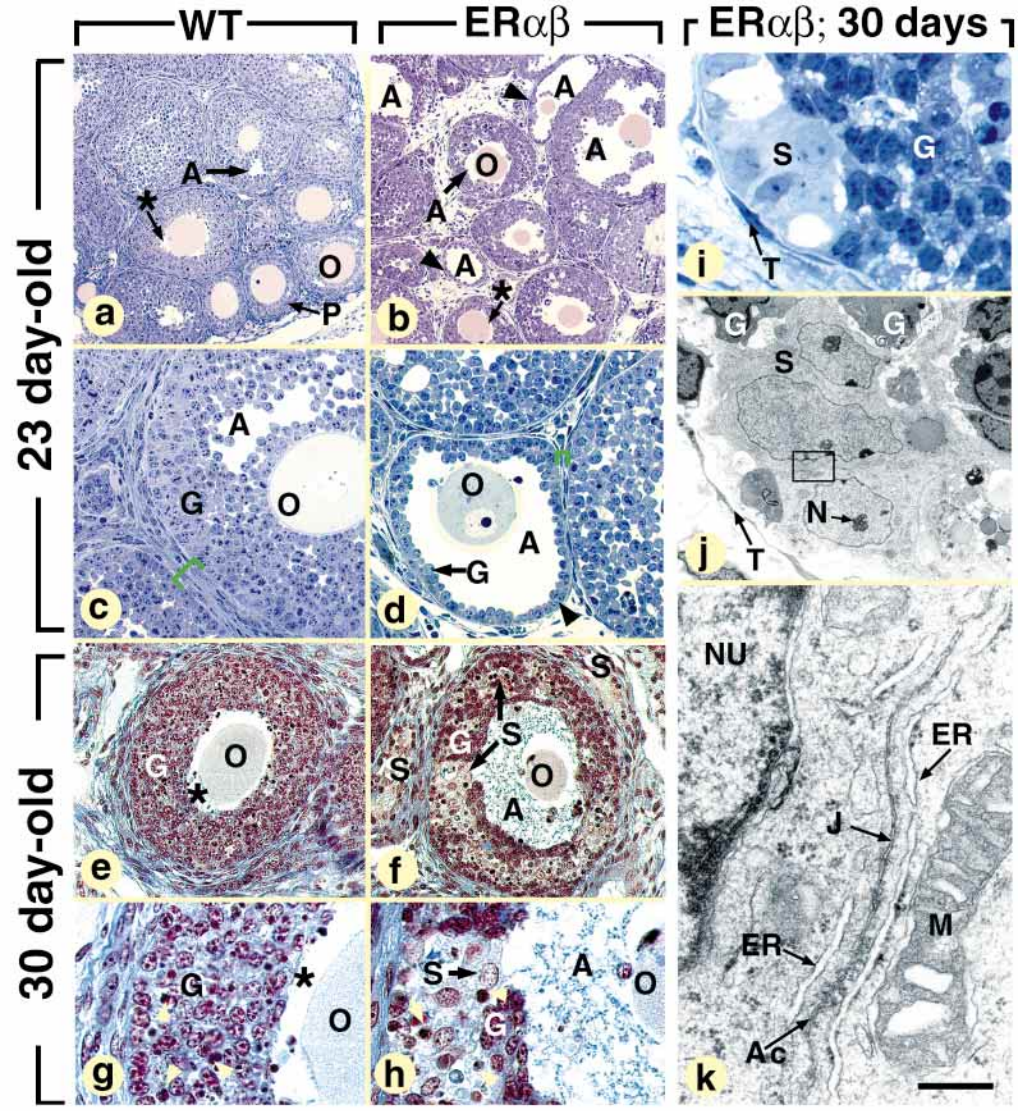

Fig. 5. Histological and thin sections of WT and ERαβKO (ERαβ) ovaries before puberty (a-d) and at the onset of puberty (e-k). (a-d) Semi-thin sections and (e-h) paraffin-embedded ovaries. (g) and (h) are higher magnification views of (e) and (f), respectively. (i) Semi-thin section of the follicular wall. (j) Thin section adjacent to (i). (k) Ectoplasmic specialization contained within the box in (j). The green brackets in panels (c) and (d) encompass the theca of two adjacent follicles. Yellow arrowheads in panels (g,h) point to apoptotic cells. Black arrowheads in panels (b,d) point to abnormal antral follicles displaying a single layer of granulosa cells. Asterisks in panels (a,b,e,g) indicate an artefactual detachment of the oocyte from the follicular wall due to cell retraction caused by tissue processing. Scale bar: 150 μm in a,b; 55 μm in c-f; 25 μm in g,h; 20 μm in i; 5 μm in j; 0.5 μm in k.

AMH in adult ERαβKO ovaries were conspicuously fewer than in WT ovaries, an observation that is in keeping with a marked increase in number of atretic follicles in these mutant ovaries.

In the normal male, expression of AMH, one of the earliest marker of Sertoli cells, is high in the fetus then decreases progressively after birth to reach background levels prior to the completion of puberty (Münsterberg and Lovell-Badge, 1991). In ERαβKO mice, immunostaining for AMH of ovarian Sertoli cells, which was only faint in post-pubertal ovaries (S, Fig. 7e) and undetectable in adult ovaries (T and C, Fig. 7c), does not appear to recapitulate that observed during normal Sertoli cell differentiation.

Ovarian response of ERαKO, ERβKO and ERαβKO compound mutants to exogenous gonadotropins

To gain further insight into the infertility or reduced fertility, as well as in defects in follicle maturation observed in the ER mutant mice, 21-25-day-old prepubertal mutant and WT mice were treated with gonadotropins to stimulate ovulation. The average yield of oocyte per female was similar in WT,

Table 2. Oocytes produced after superovulation of WT, ERβ$^{+/-}$ and ERα$^{+/-}$/ERβ$^{+/-}$ females (used as controls), and ERαKO, ERβKO, ERα$^{+/-}$/ERβKO and ERαβKO mutant females (21-25 days old)

		Oocyte count		
Genotype	*n*	Average		Range
WT	9	37.00±10.39	35.55±4.53	0-87
ERβ$^{+/-}$	14	28.79±6.34		1-80
ERα$^{+/-}$/ERβ$^{+/-}$	8	45.75±6.68		21-76
ERαKO	3	0		–
ERαKO/ERβ$^{+/-}$	4	1.00		0-4
ERβKO (A)	13	17.62±3.59*		4-48
ERβKO (B)	16	0		–
ERα$^{+/-}$/ERβKO	11	0.18		0-2
ERαβKO	3	0		–

The response of WT, ERβ$^{+/-}$ and ERα$^{+/-}$/ERβ$^{+/-}$ females are not statistically different. Two types of response were observed for ERβKO females: (A) responded to superovulation, whereas group (B) had no ovulation. The number of oocytes is presented as mean±s.e.m.

*Statistically different from control females (P=0.019; unpaired t-test).

ERβ$^{+/-}$ and ERα$^{+/-}$/ERβ$^{+/-}$ mutants (Table 2). In contrast, superovulation was drastically reduced in ERαKO and ERαKO/ERβ$^{+/-}$ females, as only one of these seven females produced four oocytes, while the others (86%) did not appear to ovulate at all (Table 2, and data not shown). This is at variance with the data obtained with αERKO mutants in which up to 83% of the ERα females superovulated, albeit with a reduced oocyte yield (Couse et al., 1999a; Rosenfeld et al., 2000).

Interestingly, hormonally treated ERβKO females responded according to two modes. Approximately half of them did not yield detectable ova, while the others exhibited a reduced yield of oocyte per female (Table 2). This is also at variance with the previous data of Krege et al. (1998) who reported that more than 80% of their βERKO females superovulated, albeit with reduced oocyte yields. Strikingly, the introduction of one disrupted ERα allele into the ERβKO background (ERα$^{+/-}$/ERβKO mutants) fully abrogated the variability in penetrance observed for the superovulation defect in ERβKO mice. Finally, as expected, no ova could be collected from 'superovulated' ERαβKO females.

As expected, superovulation treatment of WT prepubertal females induced the formation of multiple corpora lutea (CL, compare Fig. 6a with 6d). Ovaries from superovulated ERαKO and ERαKO/ERβ$^{+/-}$ appeared almost filled with healthy unruptured preovulatory follicles (OV, Fig. 6f,i, and data not shown), defined by their broad antrum (A), separation of the cumulus oophorus (CU) from the rest of the follicular epithelium and loose connection of the cumulus oophorus with the oocyte (Parkes, 1960). Similar preovulatory follicules were observed in ovaries of WT mice sacrificed shortly (i.e., seven hours) after hCG injection (Fig. 6h). Ovaries from the ERβKO and ERα$^{+/-}$/ERβKO mice that failed to ovulate in response to exogenous gonadotropins (Fig. 6g,j, and data not shown) contained numerous large follicles whose antrum were, however, conspicuously less developed than that of preovulatory follicles, and which had not achieved their maturation as their oocyte remained attached to the follicular wall via the cumulus oophorus (Fig. 6j, compare with Fig. 6h,i; and data not shown). Superovulation treatment of ERαβKO mice induced the growth of the antral follicles (compare SA and LA in Fig. 6c and 6e), but never up to the preovulatory stage (compare Fig. 6e with 6f).

Luteal cells were not observed in ERαKO, ERαKO/ERβ$^{+/-}$, ERα$^{+/-}$/ERβKO and ERαβKO ovaries, nor in those of ERβKO mice with anovulation. Therefore, prepubertal WT and ERαKO ovaries respond to stimulation by exogenous gonadotropins by the production of preovulatory follicles, whereas, upon similar stimulation, complete follicular maturation was not achieved in some ERβKO and in all ERα$^{+/-}$/ERβKO and ERαβKO ovaries.

Testis and male urogenital tract in ERαβKO mutants

In agreement with previously published results (Eddy et al., 1996; Hess et al., 1997; Couse et al., 1999b), the testis of our ERαKO and ERαβKO adult males showed a loss of germ cells in the seminiferous tubules, and a marked dilation of straight

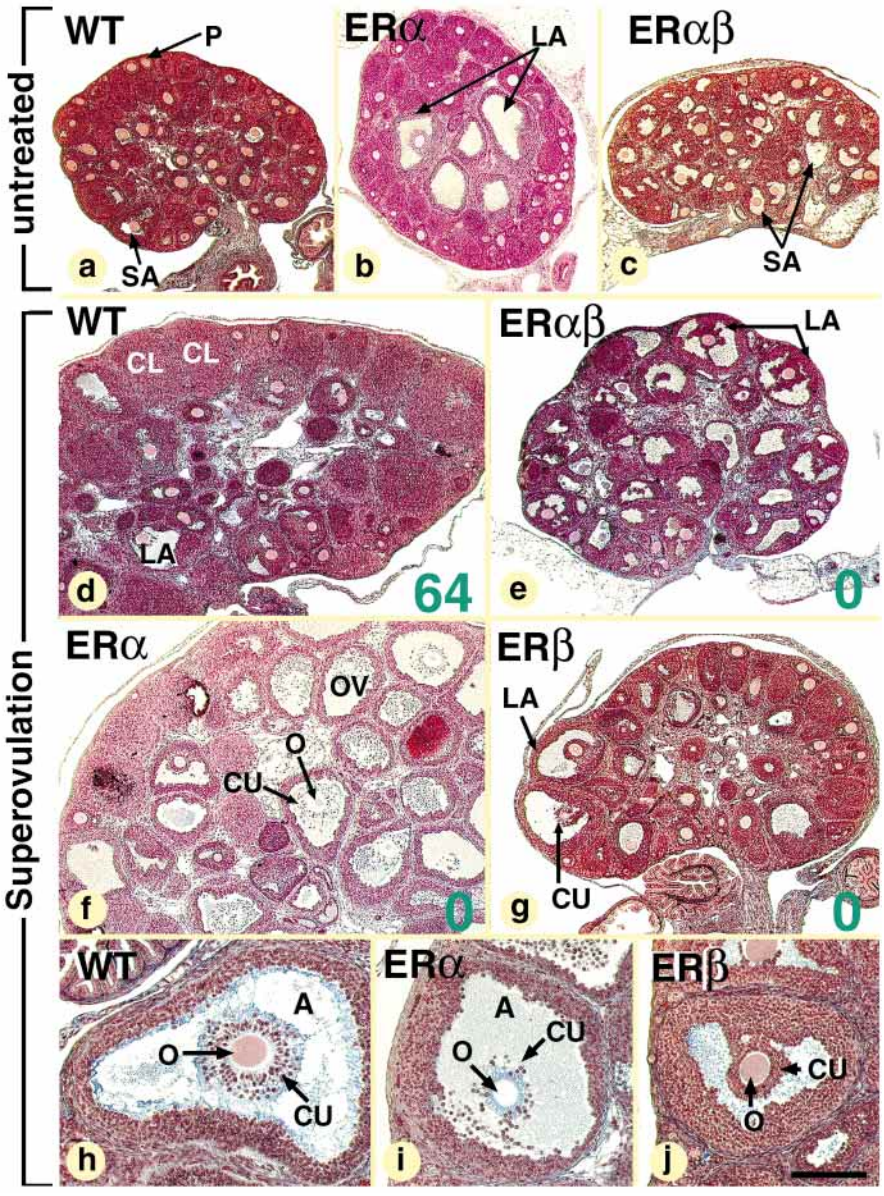

Fig. 6. Ovaries from 23-day-old prepubertal WT, ERαKO (ERα), ERβKO (ERβ) and ERαβKO (ERαβ) mice without (a-c) or with superovulation treatment (d-j). The number of eggs recovered in the oviducts of each superovulated mouse is indicated at the lower right corner of the micrographs in (d-g). (h-j) are representative views of large follicles observed prior (h) or after (i,j) the expected time of ovulation. A, antrum; CL, corpora lutea; CU, cumulus oophorus; LA, large antral follicles; O, oocyte; P, primary follicles; SA, small antral follicles. Scale bar: 400 μm in a-g; 145 μm in h-j.

tubules and rete testis (results not shown). As reported for βERKO mice (Krege et al., 1998), testes of our ERβKO mice were normal. However, in contrast to data presented in this previous βERKO report, we did not find any histological sign of hyperplasia in the (ventral, dorsolateral and cranial) prostate lobes and urinary bladder of 12- (*n*=2) and 20- (*n*=4) month-old ERβKO males (Fig. 8a-d, and data not shown). Moreover, the different lobes of the prostate, the seminal vesicles and the urinary bladder of 8-month-old ERαβKO males (*n*=3) were histologically indistinguishable from their counterparts in age-matched WT littermates (SV, CP and DP, Fig. 8e-h, and data not shown). Detection of the cell proliferation-associated nuclear antigen Ki-67 showed only rare labeled nuclei in all prostate lobes of WT mice at 8 and 20 months of age, and the number of labeled nuclei was not increased in the same tissues of ERαβKO mice and ERβKO mice analysed at 8 and 20 months, respectively (Fig. 8i,j; and data not shown).

The cell proliferation rate in the prostate of 20-month-old ERβKO and of 8-month-old ERαβKO mutants was assessed by BrdU incorporation into S phase nuclei and compared with that of age-matched WT males. BrdU-labeled nuclei were rare in all three prostate lobes of control males, as well as in those of ER mutant males. Labeling indices were as follow: cranial prostate, 0.25%±0.1 for control (*n*=6) versus 0.22%±0.02 for ERβKO males (*n*=4) and 0.11% for ERαβKO males (*n*=2); dorsal prostate, 0.14%±0.05 for control versus 0.09%±0.02 for ERβKO and 0.08% for ERαβKO males; ventral prostate, 0.41%±0.13 for control versus 0.47%±0.18 for ERβKO and 0.18% for ERαβKO males.

DISCUSSION

Partial functional redundancy between ERβ and ERα in ovarian follicle growth, ovulation and interstitial cell development.

The actions of estrogen on ovarian follicle growth are not fully understood (Couse and Korach, 1999; Rosenfeld et al., 2000; and references therein). Studies of hypophysectomized rats and mutant mice lacking follicle-stimulating hormone (FSH) or its receptor (FSHR) have shown that early stages of folliculogenesis are independent on both steroids and gonadotropins, whereas estradiol and FSH exert synergistic stimulatory effects on the proliferation of granulosa cells from preantral follicles (Dierich et al., 1998; reviewed in Robker and Richards, 1998b). The arrest in follicle growth after the beginning of antrum formation in ERαβKO mice (present report) shows, at the very least, that signaling through ERs is necessary to complete folliculogenesis.

In WT rodent ovary, ERβ is the predominant estrogen receptor expressed in granulosa cells (Byers et al., 1997; Sar and Welsch, 1999; Schomberg et al., 1999). However, granulosa cells appear normal in ERβKO mice, and the rarity or absence of corpora lutea in the ovaries of most adult ERβ null mutant mice (Krege et al., 1998, and present results) represents the only evidence that folliculogenesis might be impaired. Healthy large antral follicles are present in the ovaries of ERαKO adults, whereas ovarian follicles at the large antral stage exhibit a conspicuous deficiency in granulosa cells in $ER\alpha^{+/-}$/ERβKO and ERαβKO adults. Interestingly, a similar phenotype is observed in follicles that are deficient in cyclin D2, an FSH-responsive gene which is involved in granulosa cell proliferation (Sicinski et al., 1996). Altogether, these data indicate that (1) signaling through ERs is required for the proliferation of granulosa cells, (2) ERα is mostly dispensable for folliculogenesis, whereas (3) the apparent dispensability of ERβ in this process likely reflects a functional compensation of ERβ inactivation by ERα (functional redundancy).

As transgenic overexpression of luteinizing hormone (LH) causes premature formation of antral follicles, the known elevation of endogenous LH levels before the expected time of puberty in ERα knockout mutants (Couse et al, 1999a), and most probably in ERα/ERβ double knockout mutants, suffices to account for precocious antrum formation in their ovaries. Aside from promoting antrum formation, excess LH increases serum estradiol (Risma et al., 1997). As LH per se does not promote granulosa cell proliferation (Robker and Richards, 1998a,b), the large number of granulosa cells in the prematurely developed large follicles of mice overexpressing

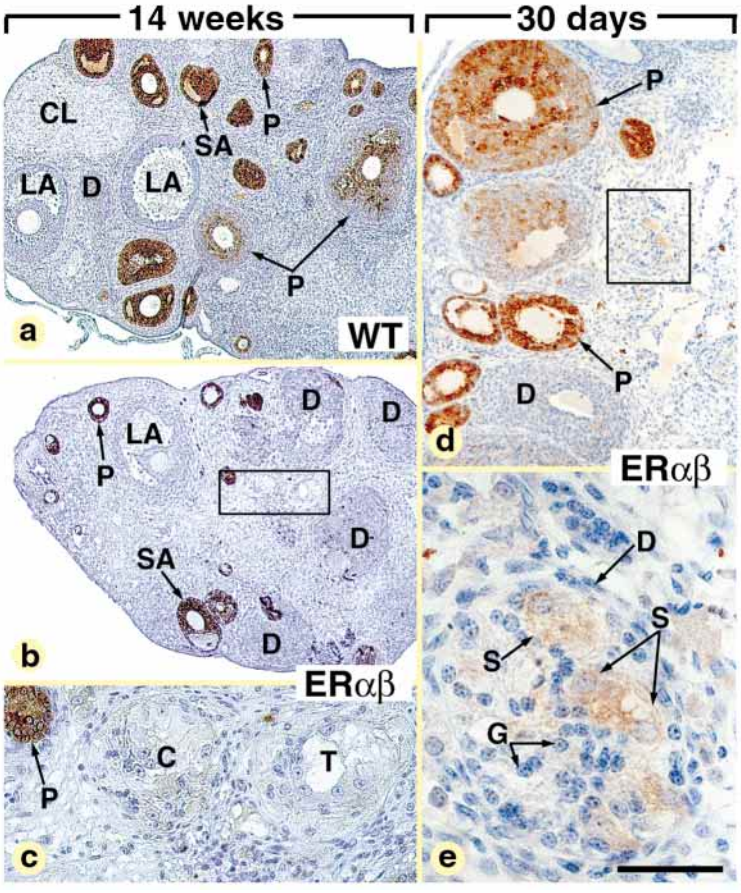

Fig. 7. Anti-Müllerian hormone (AMH) immunostaining of WT (a) and ERαβKO (b-e) ovaries at 30 days (a-c) and 14 weeks (d,e). (c,e) are high-magnification of boxes in (b,d), respectively. C, Sertoli cell cluster; CL, corpus luteum; D, degenerating follicles; G, granulosa cells; LA, large antral follicles; P, primary follicles; S, Sertoli cells; SA, small antral follicle; T, Sertoli cell tubule. Scale bar: 540 μm in a,b; 120 μm in c; 200 μm in d; 40 μm in e.

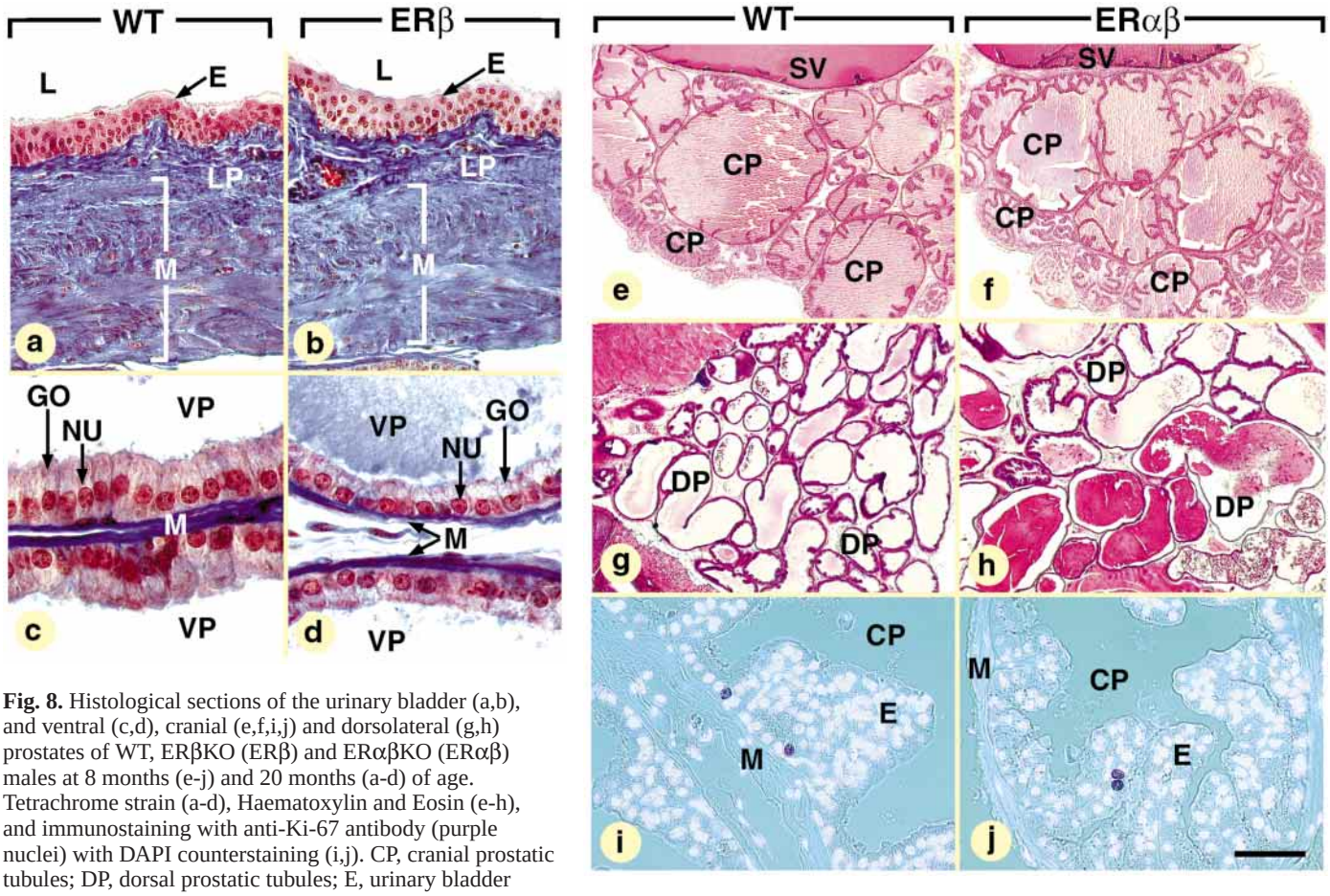

Fig. 8. Histological sections of the urinary bladder (a,b), and ventral (c,d), cranial (e,f,i,j) and dorsolateral (g,h) prostates of WT, ERβKO (ERβ) and ERαβKO (ERαβ) males at 8 months (e-j) and 20 months (a-d) of age. Tetrachrome strain (a-d), Haematoxylin and Eosin (e-h), and immunostaining with anti-Ki-67 antibody (purple nuclei) with DAPI counterstaining (i,j). CP, cranial prostatic tubules; DP, dorsal prostatic tubules; E, urinary bladder epithelium; GO, region of the Golgi apparatus; L, lumen of the urinary bladder; LP, lamina propia; M, smooth muscles; Nu, nuclei; SV, seminal vesicle; VP, ventral prostatic tubule. Scale bar: 60 μm in a,b; 25 μm in c,d; 250 μm in e-h; 45 μm in i,j.

LH (Risma et al., 1997) or lacking ERα (present report) is likely to reflect estradiol-induced mitogenic effects (reviewed in Robker and Richards, 1998b). In contrast, ERαβKO prepubertal antral follicles are markedly deficient in granulosa cells. Therefore, the proliferative response of prepubertal granulosa cells to estrogens could be mediated by ERβ.

Following administration of exogenous gonadotropins, approximately half of our prepubertal ERβKO mice fail to form preovulatory follicles, supporting the conclusion that ERβ indeed plays an essential role in mediating the stimulatory effects of estrogens on granulosa cell proliferation. However, half of our prepubertal ERβKO mice ovulate following administration of gonadotropins. As all 'superovulated' ERα$^{+/-}$/ERβKO mice are unable to form preovulatory follicles, functional compensation of ERβ inactivation by ERα within the ovary provides the simplest explanation to account for the existence of two groups of prepubertal ERβKO mice differing in their response to gonadotropin treatment. This functional compensation (redundancy) may be cell autonomous (Tetsuka et al., 1998) or involve paracrine interactions between granulosa and theca cells (Schomberg et al., 1999). Loss-of-function mutations of the human gene for ERβ have yet not been described. Such mutations could result in estrogen resistance limited to the ovary, and therefore in a state of female hypofertility whose expressivity within the same family might be subjected to considerable variations due to varying degrees of functional compensation by ERα.

Adult ERαKO ovaries are devoid of corpora lutea, similarly to αERKO mice (Lubahn et al., 1993; Schomberg et al., 1999). However, superovulation treatment of all prepubertal ERαKO and ERαKO/ERβ$^{+/-}$ females elicits the formation of a large number of follicles displaying cumulus expansion, which is the last step that can be histologically identified before follicle rupture. Therefore, even though ERα is required for follicle growth in the ovaries lacking ERβ, it appears to be dispensable for this growth in WTs, whereas it is indispensible for ovulation. Whether this effect of ERα on ovulation is mediated by the theca or interstitial cells (i.e., the main sites of ERα expression in the ovary; Schomberg et al., 1999) or components of the hypothalamic-pituitary axis expressing ERα (Kuiper et al., 1997) is unknown (see Rosenfeld et al., 2000). Interestingly, up to 83% of the αERKO mice (Lubahn et al., 1993), but only 14% of our ERαKO mice are able to superovulate (Couse et al., 1999a; Rosenfeld et al., 2000; and our present results). This discrepancy might be related to differences in genetic backgrounds. Alternatively, it could reflect the presence of a residual ERα activity in αERKO mice (Couse et al., 1995; see Results).

Interstitial glandular cells are similarly decreased in the ovarian medulla of ERαKO and ERαβKO adults. In contrast, hypertrophy of interstitial cells has been described in αERKO

mice (Schomberg et al., 1999; Couse and Korach, 1999). A possible explanation for this discrepancy could be that αERKO mice have retained some ERα activity (see above), allowing ovarian interstitial cells to respond to excess LH (Risma et al., 1997). In any event, the interstitial glandular cell deficiency in our ERαKO mice, and the normal presence of the ERα protein in these cells (Schomberg et al., 1999) strongly suggest they are primary targets of ERα action.

Involvement of mast cells in the generation of polycystic ovaries in ERαKO and ERαβKO mutant mice

In αERKO mice, the polycystic ovarian phenotype is correlated with an increase in serum LH (Couse et al., 1999a). Identical polycystic ovarian phenotypes are observed in ERαKO and ERαβKO mice showing that expression of ERβ in granulosa cells is not required to mediate the effects of supra-physiological levels of LH on the formation of follicular cysts, in contrast to a previous proposal (Couse et al., 1999a). Administration of either LH or histamine increases ovarian blood flow and capillary permeability, and causes edema of the ovarian interstitial tissue (Krishna et al., 1989; Jones et al., 1994 and references therein), and there is evidence relating cystic ovarian follicle formation with hypersecretion of either LH (Risma et al., 1995, 1997) or histamine (Hunter and Leathem, 1968). We show here that our ERαKO and ERαβKO mutants have numerous intraovarian mast cells, which is most probably associated with an increase in intraovarian histamine levels (Krishna et al., 1989 and references therein). It has recently been shown that the polycystic αERKO ovarian phenotype can be prevented by decreasing the serum LH levels to within the wild-type range through treatment with Antide, a gonadotropin-releasing hormone antagonist (Couse et al., 1999a). It is noteworthy, however, that (1) Antide per se can interfere with histamine secretion from mast cells (Ljungqist et al., 1988) and (2) administration of LH can increase mast-cell number in the ovary (Jones et al., 1994). It is therefore possible that locally increased histamine levels participate to the formation of follicular cysts and edema of the interstitial tissue of our ERαKO and ERαβKO ovaries. It would be interesting to know the status of intraovarian mast cells in ArKO mice, which, similar to ERαβKO mice, display both a block in estrogen signaling and high serum LH levels, but no polycystic ovarian phenotype (Fisher et al., 1998).

Transformation of granulosa cells into Sertoli cells in the absence of estrogen receptors

Seminiferous tubules can develop from fetal ovaries that are either (1) transplanted under the kidney capsule, (2) cultured in vitro, (3) exposed to supraphysiological concentrations of AMH in vivo or (4) lack expression of *Wnt4* (Taketo-Hosotani et al., 1985; Behringer et al., 1990; Vigier et al., 1987; Vainio et al., 1999). However, the ERαβKO condition is unique in that it represents the only example of Sertoli cell differentiation occurring in a sexually mature ovary. It is noteworthy that the absence of estrogen signaling is apparently not sufficient to account for the formation of ovarian Sertoli cells, as such cells are not observed in ArKO mice that lack the capacity to synthesize estradiol (Fisher et al., 1998).

Abnormal cells present in the ovaries of αβERKO mice were characterized as Sertoli cell on the basis of their arrangement into tubular structures, their expression of AMH and SGP2, and increased *Sox9* transcripts in the whole ovary (Couse et al., 1999b). However, these features are not sufficient on their own to unambiguously identify Sertoli cells as many tumors of the mouse ovary (including adenomas, as well as granulosa cell and Sertoli cell tumors) have tubular patterns (Morgan and Alison, 1987). Moreover, AMH and SGP2 are both expressed in Sertoli and granulosa cells (Ahuja et al., 1994; Aronow et al., 1993; Münsterberg and Lovell-Badge, 1991; Hirobe et al., 1992 and references therein), and *Sox9* transcripts are present in WT ovary (Couse et al., 1999b). In contrast, ectoplasmic specializations evidenced in ERαβKO ovaries (present report) correspond to intercellular cell junctions that, in the male, form the blood-testis barrier and are specific to Sertoli cells (Pelletier and Byers, 1992).

In αβERKO ovaries (Couse et al, 1999b), Sertoli cells are all organized into spherical structures resembling follicles and they begin to differentiate within preantral follicles. In contrast, in our ERαβKO mice, the majority of the ovarian Sertoli cells form irregular clusters (Fig. 3g,k, and data not shown), and these cells develop within the granulosa cell layers of follicles at advanced stage of atresia, most of which have already lost their spherical shape (as well as their oocyte) and exhibit leakage of their epithelial cells in the interstitial tissue. One possibility would be that Sertoli cells escaping from atretic follicles give rise to irregular aggregates, whereas those remaining within the limits of the follicular basement membrane form tubular structures. In any event, in our ERαβKO mice, Sertoli cell differentiation is clearly correlated with follicular atresia. Moreover, the observation that oocyte loss can lead to sex reversal of follicular cells (Vainio et al., 1999 and references therein) suggests that granulosa cells lacking ERs may be biased towards a Sertoli cell fate that becomes obvious only following the death of the oocyte.

In ERαβKO ovaries, all cells synthesizing large amounts of AMH possess morphological features of granulosa cells, whereas expression of AMH in ovarian Sertoli cells is low or absent. These data strongly suggest that ERαβKO ovarian Sertoli cells are derived, by metaplastic transformation, from AMH-expressing granulosa cells rather than from a bipotent precursor present within the follicular epithelium. Additionally, immunohistochemical analysis of ERαβKO ovaries shows that the number of stained follicles is reduced: the increase in AMH mRNA levels in αβERKO ovaries reported by Couse et al. (1999b) is apparently not reflected at the protein level. It seems therefore unlikely that an elevation of AMH levels is the cause of the Sertoli cell differentiation occurring in ovaries lacking ERs.

A function for ERβ in female genital tract

As already mentioned, the incomplete penetrance of impaired follicular growth in ERβKO ovaries probably reflects the existence of a partial functional compensation by ERα, which may be expressed at low levels in granulosa cells (Tetsuka et al., 1998). Inversely, our data indicate that, although ERα is the predominant ER expressed in the uterus and vagina, ERβ could partially compensate for the loss of ERα in the genital tract, as the ERαKO uterine and vaginal hypoplasia is exacerbated in ERαβKO mice, whereas the ERβKO genital tract appears normal. This possibility is in keeping with the

detection of low levels of ERβ transcripts and proteins in the uterus and vagina in both WT and αERKO mice (Couse et al., 1997; Wang et al., 1999). The lack of effect of ERβ inactivation on the genital tract of αERKO mice (Couse et al., 1999b) supports the possibility of a persistent ERα activity in αβERKO mice (Couse et al., 1995).

Inactivation of ERβ does not elicit hyperplasia of the urinary bladder and prostate gland epithelia

Estrogens have been implicated in the pathogenesis of benign prostatic hyperplasia (reviewed in Habenicht et al., 1993), as well as in prostatic carcinogenesis and tumor progression (Bonkhoff et al., 1999 and references therein). ERα and ERβ mRNA are present in approximately equal amounts in the mouse prostate (Couse et al., 1997). In addition, the ERβ protein is present at apparently high levels in the epithelium of the mouse urinary bladder (Rosenfeld et al., 1998). In this context, it is noteworthy that our data do not confirm the previously reported epithelial hyperplasia of the urinary bladder and prostate ducts in βERKO mutants (Krege et al., 1998). Moreover, in old ERαβKO males, we did not observe any significant increased cell proliferation in these epithelia.

We are grateful to Dr N. Josso and Dr R. Rey (ENS, INSERM) for the gift of anti-AMH antibody. We thank C. Dennefeld, M. Duval, J.M. Garnier, C. Gérard, S. Roth and I. Tilly for their expert technical assistance; all of the members of the monoclonal antibody, the oligonucleotide, the sequencing, the ES cell culture, the microinjection and the animal facilities; the secretarial staff for typing; and the illustration staff for preparing the figures. Special thanks go to Dr D. Metzger and Dr M. LeMeur for experimental support and helpful discussion. This work was supported by grants from the Centre National de la Recherche Scientifique, the Institut National de la Santé et de la Recherche Médicale, the Collège de France, the Institut Universitaire de France, the Hôpital Universitaire de Strasbourg, the Association pour la Recherche sur le Cancer, and the Fondation pour la Recherche Médicale.

REFERENCES

Adra, C. N., Boer, P. H. and McBurney, M. W. (1987). Cloning and expression of the mouse pgk-1 gene and the nucleotide sequence of its promoter. *Gene* **60**, 65-74.

Ahuja, H. S., Tenniswood, M., Lockshin, R. and Zakeri, Z. F. (1994). Expression of clusterin in cell differentiation and cell death. *Biochem. Cell. Biol.* **72**, 523-530.

Al-Attar, L., Noël, K., Dutertre, M., Belville, C., Forest, M. G., Burgoyne, P. S., Josso, N. and Rey, R. (1997). Hormonal and cellular regulation of Sertoli cell anti-Müllerian hormone production in the postnatal mouse. *J. Clin. Invest.* **100**, 1335-1343.

Aronow, B. J., Lund, S. D., Brown, T. L., Harmony, J. A. K. and Witte, D. P. (1993). Apolipoprotein J expression at fluid-tissue interfaces: potential role in barrier cytoprotection. *Proc. Natl. Acad. Sci. USA* **90**, 725-729.

Auffray, C. and Rougeon, F. (1980). Purification of mouse immunoglobulin heavy-chain messenger RNAs from total myeloma tumor RNA. *Eur. J. Biochem.* **107**, 303-314.

Baarends, W. M., Uilenbroek, J. T. J., Kramer, P., Hoogerbrugge, J. W., van Leeuwen, E. C. M., Themmen, A. P. N. and Grootegoed, J. A. (1995). Anti-müllerian hormone and anti-müllerian hormone type II receptor messenger ribonucleic acid expression in rat ovaries during postnatal development, the estrous cycle, and gonadotropin-induced follicle growth. *Endocrinology* **136**, 4951-4962.

Behringer, R. R., Cate, R. L., Froelick, G. J., Palmiter, R. D. and Brinster, R. L. (1990). Abnormal sexual development in transgenic mice chronically expressing müllerian inhibiting substance. *Nature* **345**, 167-170.

Berry, M., Metzger, D. and Chambon, P. (1990). Role of the two activating domains of the oestrogen receptor in the cell-type and promoter-context dependent agonistic activity of the anti-oestrogen 4-hydroxytamoxifen. *EMBO J.* **9**, 2811-2818.

Bonkhoff, H., Fixemer, T., Hunsicker, I. and Remberger, K. (1999). Estrogen receptor expression in prostate cancer and premalignant prostatic lesions. *Am. J. Pathol.* **155**, 641-647.

Byers, S., Pelletier, R. M. and Suárez-Quian, C. (1993). Sertoli-Sertoli cell junctions and the seminiferous epithelium barrier. In *The Sertoli Cell* (ed. L. D. Russell and M. D. Griswold), pp. 431-446. Clearwater: Cache River Press.

Byers, M., Kuiper, G. G., Gustafsson, J. A. and Park-Sarge, O. K. (1997). Estrogen receptor-β mRNA expression in rat ovary: down-regulation by gonadotropins. *Mol. Endocrinol*. **11**, 172-182.

Couse, J. F., Curtis, S. W., Washburn, T. F., Lindzey, J., Golding, T. S., Lubahn, D. B., Smithies, O. and Korach, K. S. (1995). Analysis of transcription and estrogen insensitivity in the female mouse after targeted disruption of the estrogen receptor gene. *Mol. Endocrinol*. **9**, 1441-1454.

Couse, J. F., Lindzey, J., Grandien, K., Gustafsson, J. A. and Korach, K. S. (1997). Tissue distribution and quantitative analysis of estrogen receptor-α (ERα) and estrogen receptor-β (ERβ) messenger ribonucleic acid in the wild-type and ERα-knockout mouse. *Endocrinology* **138**, 4613-4621.

Couse, J. F. and Korach, K. S. (1999). Estrogen receptor null mice: what have we learned and where will they lead us ? *Endocr. Rev.* **20**, 358-417.

Couse, J. F., Bunch, D. O., Lindzey, J., Schomberg, D. W. and Korach, K. S. (1999a). Prevention of the polycystic ovarian phenotype and characterization of ovulatory capacity in the estrogen receptor-α knockout mouse. *Endocrinology* **140**, 5855-5865.

Couse, J. F., Curtis Hewitt, S., Bunch, D. O., Sar, M., Walker, V. R., Davis, B. J. and Korach, K. S. (1999b). Postnatal sex reversal of the ovaries in mice lacking estrogen receptors α and β. *Science* **286**, 2328-2331.

Dierich, A. and Dollé, P. (1997). Gene targeting in embryonic stem cells. In *Developmental Toxicology and Biology* (ed. R. Thiel and S. Klug), pp. 111-123. Oxford: Blackwell Science.

Dierich, A., Sairam, M. R., Monaco, L., Fimia, G. M., Gansmuller, A., LeMeur, M. and Sassone-Corsi, P. (1998). Impairing follicle-stimulating hormone (FSH) signaling in vivo: targeted disruption of the FSH receptor leads to aberrant gametogenesis and hormonal imbalance. *Proc. Natl. Acad. Sci. USA* **95**, 13612-13617.

Dupé, V., Davenne, M., Brocard, J., Dollé, P., Mark, M., Dierich, A., Chambon, P. and Rijli, F. M. (1997). In vivo functional analysis of the Hoxa-1 3′ retinoic acid response element (3′RARE). *Development* **124**, 399-410.

Eddy, E. M., Washburn, T. F., Bunch, D. O., Goulding, E. H., Gladen, B. C., Lubahn, D. B. and Korach, K. S. (1996). Targeted disruption of the estrogen receptor gene in male mice causes alteration of spermatogenesis and infertility. *Endocrinology* **137**, 4796-4805.

Fawcett, D. W. (1986). *A Textbook of Histology*. Philadelphia: Saunders.

Fisher, C. R., Graves, K. H., Parlow, A. F. and Simpson, E. R. (1998). Characterization of mice deficient in aromatase (ArKO) because of targeted disruption of the cyp19 gene. *Proc. Natl. Acad. Sci. USA* **95**, 6965-6970.

Ghyselinck, N. B., Båvik, C., Sapin, V., Mark, M., Bonnier, D., Hindelang, C., Dierich, A., Nilsson, C. B., Håkansson, H., Sauvant, P., Azaïs-Braesco, V., Frasson, M., Picaud, S. and Chambon, P. (1999). Cellular retinol-binding protein I is essential for vitamin A homeostasis. *EMBO J.* **18**, 4903-4914.

Green, S., Walter, P., Kumar, V., Krust, A., Bornert, J.M., Argos, P. and Chambon, P. (1986). Human oestrogen receptor cDNA: sequence, expression and homology to *v-erb-A*. *Nature* **320**, 134-139.

Gronemeyer, H. and Laudet, V. (1995). Transcription factors 3: nuclear receptors. In *Protein Profile.* Vol. 2. (ed. P. Sheterline), pp. 1173-1308. Liverpool: Academic Press.

Habenicht, U. F., Tunn, U. W., Senge, T., Schröder, F. H., Schweikert, H. U., Bartsch, G. and El Etreby, M. F. (1993). Management of benign prostatic hyperplasia with particular emphasis on aromatase inhibitors. *J. Steroid Biochem. Mol. Biol*. **44**, 557-563.

Harrison, R. J. and Weir, B. J. (1977). Structure of the mammalian ovary. In *The Ovary* (ed. L. Zuckemann and B. J. Weir), pp. 113-217. New York: Academic Press.

Hess, R. A., Bunick, D., Lee, K. H., Bahr, J., Taylor, J. A., Korach, K. S. and Lubahn, D. B. (1997). A role for oestrogens in the male reproductive system. *Nature* **390**, 509-512.

Hirobe, S., He, W. W., Lee, M. M. and Donahoe, P. K. (1992). Müllerian

inhibiting substance messenger ribonucleic acid expression in granulosa and Sertoli cells coincides with their mitotic activity. *Endocrinology* **131**, 854-862.

Hogan, B., Beddington, R., Costantini, F. and Lacy, E. (1994). *Manipulating the Mouse Embryo, a Laboratory Manual.* New York: Cold Spring Harbor Laboratory Press.

Hunter, F. and Leathem, J. H. (1968). Histamine concentrations in normal and cystic rat ovaries. *Endocrinology* **82**, 171-172.

Jones, R. E., Duvall, D., Guillette, L. J., Lopez, Jr. and Lopez, K. H. (1994). Number and state of rat ovarian mast cells after exogenous administration of luteinizing hormone. *Comp. Biochem. Physiol*. **108**, 555-559.

Kato, S., Endoh, H., Masuhiro, Y., Kitamoto, T., Uchiyama, S., Sasaki, H., Masushige, S., Gotoh, Y., Nishida, E., Kawashima, H., Metzger, D., Chambon, P. (1995). Activation of the estrogen receptor through phosphorylation by mitogen-activated protein kinase. *Science* **270**, 1491-1494.

Krege, J. H., Hodgin, J. B., Couse, J. F., Enmark, E., Warner, M., Mahler, J. F., Sar, M., Korach, K. S., Gustafsson, J. A. and Smithies, O. (1998). Generation and reproductive phenotypes of mice lacking estrogen receptor *β. Proc. Natl. Acad. Sci. USA* **95**, 15677-15682.

Krishna, A., Beesley, K. and Terranova, P. F. (1989). Histamine, mast cells and ovarian function. *J. Endocrinol*. **120**, 363-371.

Krust, A., Green, S., Argos, P., Kumar, V., Walter, P., Bornert, J.M. and Chambon, P. (1986). The chicken oestrogen receptor sequence: homology with *v-erbA* and the human oestrogen and glucocorticoid receptors. *EMBO J.* **5**, 891-897.

Kuhn, E. M. and Therman, E. (1988). The behavior of heterochromatin in mouse and human nuclei. *Cancer Genet. Cytogenet*. **34**, 143-351.

Kuiper, G. G., Enmark, E., Pelto-Huikko, M., Nilsson, S. and Gustafsson, J. A. (1996). Cloning of a novel receptor expressed in rat prostate and ovary. *Proc. Natl. Acad. Sci. USA* **93**, 5925-5930.

Kuiper, G. G., Carlsson, B., Grandien, K., Enmark, E., Häggblad, J., Nilsson, S. and Gustafsson, J. A. (1997). Comparison of the ligand binding specificity and transcript tissue distribution of estrogen receptors α and β. *Endocrinology* **138**, 863-870.

Ljungqvist, A., Feng, D. M., Hook, W., Shen, Z. X., Bowers, C. and Folkers, K. (1988). Antide and related antagonists of luteinizing hormone release with long action and oral activity. *Proc. Natl. Acad. Sci USA* **85**, 8236-8240.

Lu, B., Leygue, E., Dotzlaw, H., Murphy, L. J., Murphy, L. C. and Watson, P. H. (1998). Estrogen receptor-β mRNA variants in human and murine tissues. *Mol. Cell. Endocrinol.* **138**, 199-203.

Lubahn, D. B., Moyer, J. S., Golding, T. S., Couse, J. F., Korach, K. S. and Smithies, O. (1993). Alteration of reproductive function but not prenatal sexual development after insertional disruption of the mouse estrogen receptor gene. *Proc. Natl. Acad. Sci. U S A* **90**, 11162-11166.

Lufkin, T., Dierich, A., LeMeur, M., Mark, M. and Chambon, P. (1991). Disruption of the Hox-1.6 homeobox gene results in defects in a region corresponding to its rostral domain of expression. *Cell* **66**, 1105-1119.

Metzger, D., Clifford, J., Chiba, H. and Chambon, P. (1995). Conditional site-specific recombination in mammalian cells using a ligand-dependent chimeric Cre recombinase. *Proc. Natl. Acad. Sci. USA* **92**, 6991-6995.

Morgan, K. T. and Alison, R. H. (1987). Tubular adenoma, ovary, mouse. In *Genital System* (ed. R. D. Hunt, U. Mohr and T. C. Jones), pp. 36-41, Berlin: Springer Verlag.

Mosselman, S., Polman, J., Dijkema, R. (1996). ERβ: identification and characterization of a novel human estrogen receptor. *FEBS Lett.* **392**, 49-53.

Mossman, H. W. and Duke, K. L. (1973). Some comparartive aspects of the mammalian ovary. In *Handbook of Physiology* (ed. R. Greep), Part 2, 389-402, Baltimore: Williams and Wilkins.

Münsterberg, A. and Lovell-Badge, R. (1991). Expression of the mouse anti-müllerian hormone gene suggests a role in both male and female sexual differentiation. *Development* **113**, 613-624.

Muramatsu M. and Inoue S. (2000). Estrogen receptors: how do they control reproductive and nonreproductive functions ? *Biochem. Biophys. Res. Commun.* **270**, 1-10.

Parkes, A. S. (1960). *Marshall's Physiology of Reproduction*. London: Longmans.

Paech, K., Webb, P., Kuiper, G.G., Nilsson, S., Gustafsson, J., Kushner P.J., Scanlan, T.S. (1997). Differential ligand activation of estrogen receptors ERα and ERβ at AP1 sites. *Science* **277**, 1508-1510.

Pelletier, R. M. and Byers, S. W. (1992). The blood-testis barrier and Sertoli cell junctions: structural considerations. *Microsc. Res. Tech*. **20**, 3-33.

Risma, K. A., Clay, C. M., Nett, T. M., Wagner, T., Yun, J. and Nilson, J. H. (1995). Targeted overexpression of luteinizing hormone in transgenic mice leads to infertility, polycystic ovaries, and ovarian tumors. *Proc. Natl. Acad. Sci. USA* **92**, 1322-1326.

Risma, K. A., Hirshfield, A. N. and Nilson, J. H. (1997). Elevated luteinizing hormone in prepubertal transgenic mice causes hyperandrogenemia, precocious puberty, and substantial ovarian pathology. *Endocrinology* **138**, 3540-3547.

Robker, R. L. and Richards, J. S. (1998a). Hormone-induced proliferation and differentiation of granulosa cells: a coordinated balance of the cell cycle regulators cyclin D2 and $p27^{Kip1}$. *Mol. Endocrinol.* **12**, 924-940.

Robker, R. L. and Richards, J. S. (1998b). Hormonal control of the cell cycle in ovarian cells: proliferation versus differentiation. *Biol. Reprod.* **59**, 476-482.

Rochette-Egly, C., Lutz, Y., Pfister, V., Heyberger, S., Scheuer, I., Chambon, P. and Gaub, M. P. (1994). Detection of retinoid X receptors using specific monoclonal and polyclonal antibodies. *Biochem. Biophys. Res. Commun*. **204**, 525-536.

Rosenfeld, C. S., Ganjam, V. K., Taylor, J. A., Yuan, X., Stiehr, J. R., Hardy, M. P. and Lubahn, D. B. (1998). Transcription and translation of estrogen receptor-β in the male reproductive tract of estrogen receptor-α knock-out and wild-type mice. *Endocrinology* **139**, 2982-2987.

Rosenfeld, C.S., Murray, A.A., Simmer, G., Hufford, M.G., Smith, M.F., Spears, N. and Lubahn, D.B. (2000). Gonadotropin induction of ovulation and corpus luteum formation in young estrogen receptor-α knockout mice. *Biol. Reprod.* **62**, 599-605.

Sar, M. and Welsch, F. (1999). Differential expression of estrogen receptor-β and estrogen receptor-α in the rat ovary. *Endocrinology* **140**, 963-971.

Saville, B., Wormke, M., Wang, F., Nguyen, T., Enmark, E., Kuiper, G., Gustafsson, J-A. and Safe, S. (2000). Ligand-, cell-, and estrogen receptor subtype (α/β)-dependent activation at GC-rich (Sp1) promoter elements. *J. Biol. Chem*. **275**, 5379-5387.

Schomberg, D. W., Couse, J. F., Mukherjee, A., Lubahn, D. B., Sar, M., Mayo, K. E. and Korach, K. S. (1999). Targeted disruption of the estrogen receptor-α gene in female mice: characterization of ovarian responses and phenotype in the adult. *Endocrinology* **140**, 2733-2744.

Sicinski, P., Donaher, J. L., Geng, Y., Parker, S. B., Gardner, H., Park, M. Y., Robker, R. L., Richards, J. S., McGinnis, L. K., Biggers, J. D., Eppig, J. J., Bronson, R. T., Elledge, S. J. and Weinberg, R. A. (1996). Cyclin D2 is an FSH-responsive gene involved in gonadal cell proliferation and oncogenesis. *Nature* **384**, 470-474.

Swain, A. and Lovell-Badge, R. (1999). Mammalian sex determination: a molecular drama. *Genes Dev*. **13**, 755-767.

Taketo-Hosotani, T., Merchant-Larios, H., Thau, R. B. and Koide, S. S. (1985). Testicular cell differentiation in fetal mouse ovaries following transplantation into adult male mice. *J. Exp. Zool*. **236**, 229-237.

Tetsuka, M., Milne, M. and Hillier, S. G. (1998). Expression of oestrogen receptor isoforms in relation to enzymes of oestrogen synthesis in rat ovary. *Mol. Cell. Endocrinol*. **141**, 29-35.

Tremblay, G. B., Tremblay, A., Copeland, N. G., Gilbert, D. J., Jenkins, N. A., Labrie, F. and Giguere, V. (1997). Cloning, chromosomal localization, and functional analysis of the murine estrogen receptor β. *Mol. Endocrinol*. **11**, 353-365.

Ueno, S., Takahashi, M., Manganaro, T. F., Ragin, R. C. and Donahoe, P. K. (1989). Cellular localization of müllerian inhibiting substance in the developing rat ovary. *Endocrinology* **124**, 1000-1006.

Vainio, S., Heikkilä, M., Kispert, A., Chin, N. and McMahon, A. P. (1999). Female development in mammals is regulated by Wnt-4 signalling. *Nature* **397**, 405-409.

Vigier, B., Watrin, F., Magre, S., Tran, D. and Josso, N. (1987). Purified bovine AMH induces a characteristic freemartin effect in fetal rat prospective ovaries exposed to it in vitro. *Development* **100**, 43-55.

Wang, H., Masironi, B., Eriksson, H. and Sahlin, L. (1999). A comparative study of estrogen receptors α and β in the rat uterus. *Biol. Reprod*. **61**, 955-964.

Weber, J. E., Turner, T. T., Tung, K. S. and Russell, L. D. (1988). Effects of cytochalasin D on the integrity of the Sertoli cell (blood- testis) barrier. *Am. J. Anat.* **182**, 130-147.

White, R., Lees, J. A., Needham, M., Ham, J. and Parker, M. (1987). Structural organization and expression of the mouse estrogen receptor. *Mol. Endocrinol.* **1**, 735-744.